Practical applications for the Butterfly orbital family

Ángela Jordán*, **César Leal-Graciani**†, and **Giordana Bucchioni**§

*AUTHOR, ISAE-SUPAERO, France, angelajorci@gmail.com
†AUTHOR, ISAE-SUPAERO, France, lgmcesar8@gmail.com
§TUTOR, University of Pisa, Italy, giordana.bucchioni@ing.unipi.it

***Abstract*—The lunar mission market is experiencing significant development and growth with increasing interest from government agencies, private companies, and international collaborations. Future lunar missions are driven by scientific exploration, resource utilization, and the establishment of a sustainable human presence. The first step in order to accomplish those goals is to being able to observe and communicate with both, the Earth and the Moon in a continuous and optimized way. The work aims covering the lack of literature in practical applications for the Butterfly family by proposing three different synodic resonant butterfly orbits which could outperform the current reference orbit for the cislunar architecture, known as a Near Rectilinear Halo Orbit (NRHO), in terms of energy/time consumption.**

***Key words*—CR3BP, Earth-Moon, Butterfly Orbits, NRHO**

I. Introduction

In the near future, the lunar mission market is expected to keep growing at an accelerated pace. The Artemis program, led by NASA, is one of the primary driving forces behind this expansion. Artemis aims to return humans to the Moon by 2024 and establish a sustainable lunar presence. This ambitious program has garnered significant attention and investment, aiming to not only land astronauts on the lunar surface but also enable long-duration stays and foster scientific research and exploration. Moreover, international collaborations are also on the rise in the lunar mission market. Partnerships such as the Artemis Accords aim to establish a common vision via a practical set of principles and use of outer space to advance the Artemis Program. These activities may take place on the Moon, Mars, comets, and asteroids, as well as in orbit of the Moon or Mars, in the Lagrangian points for the Earth-Moon system [1]. These collaborations foster global participation in lunar missions and provide opportunities for scientific research, technology demonstrations, and knowledge sharing.

This endeavor's current orbit of interest is an L2 near rectilinear halo orbit (NRHO). Near rectilinear halo orbits are members of the broader set of L1 and L2 families of halo orbits. These foundational structures exist in a dynamical environment modeled in terms of multiple gravitational bodies, and the motion also persists in a higher-fidelity model. This type of trajectory was first identified in a simplified representation of the gravitational effects in the Earth–Moon system, i.e., the circular restricted three-body problem (CR3BP). In the CR3BP model, NRHOs are characterized by favorable stability properties that facilitate low-cost maintenance of NRHO like motion over long duration periods. Some NRHOs also possess favorable resonance properties that can be exploited for mission design and are particularly useful for eclipse avoidance [2].

In this investigation, the dynamical structure that bifurcates from the first period-doubling bifurcation of the NRHO region of the L2 halo family (butterfly orbits) [3] is explored to scrutinize the possible characteristics that would make a possible candidate for future lunar missions out of this orbital family.

II. Dynamical Model

The Circular Restricted Three-Body Problem (CR3BP) is a simplified mathematical model used in celestial mechanics to study the motion of a small object (such as a spacecraft) in the gravitational fields of two larger bodies, referred to as primaries, offering simplifications that facilitate easier conceptual understanding. In this problem, the two larger bodies are assumed to move in circular orbits around their center of mass. The CR3BP hypothesis assumes that the mass of the small object is negligible compared to the masses of the larger bodies, meaning that the motion of the larger bodies is unaffected by the presence of the small object. [4]

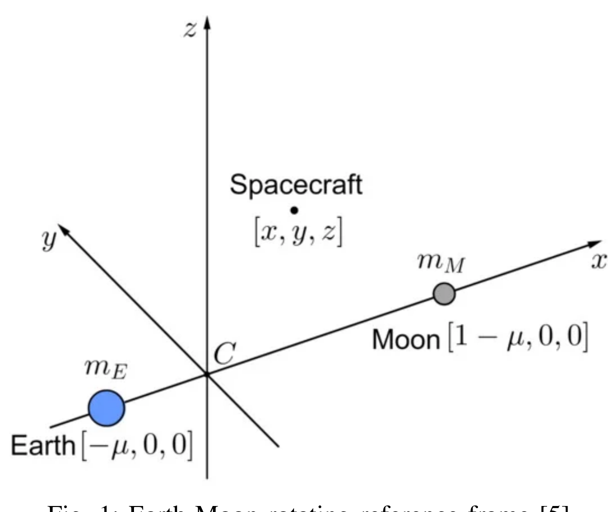

Fig. 1: Earth-Moon rotating reference frame [5]

In a coordinate system centered around the barycenter and rotating with the system (rotating or synodic frame, figure 1), the position of the negligible-mass body is denoted by (x, y, z). The x-axis points from the more extensive primary (m_1) to the smaller primary (m_2), while the z-axis is perpendicular to the orbital plane. The y-axis completes the set of orthogonal coordinates. In the CR3BP, a convention is followed to make quantities dimensionless. Normalized or nondimensional units will be used for nearly all the discussions in this paper. When appropriate, conversion to dimensional units (e.g., km, km/s, seconds) can be done to scale a problem. The following choice of units normalizes the system: the unit of mass is taken to be $m_1 + m_2$; the unit of length is chosen to be the constant separation between m_1 and m_2 (in our case the distance between the centers of the earth and the moon; $3.850 * 10^5$ km); the unit of time is chosen such that the orbital period of m_1 and m_2 around their center of mass is 2π. The universal constant of gravitation then becomes $G = 1$. It then follows that the primaries' common mean motion, n, is also unity. [6]

As a result of this dimensionless representation, the distances from the Earth and Moon to the barycenter are expressed as μ and 1 - μ, respectively. Here, the parameter μ represents the ratio of the Moon's mass to the system's total mass (μ = m_2/(m_1 + m_2)). In the specific case of the Earth-Moon system, μ is equal to 0.01215. The larger and smaller primaries are then located at (-μ, 0, 0) and (1-μ,0, 0), respectively, and the equations of motion are given by:

$$\begin{gathered} x'' = 2y' + x - (1-\mu)(x+\mu)r_1^{-3} - \mu(x-1-+\mu)r_1^{-3} \\ y'' = -2x' + y - (1-\mu)yr_1^{-3} - \mu * yr_2^{-3} \\ z'' = -(1-\mu)zr_1^{-3} - 1 - \mu * zr_2^{-3} \end{gathered} \tag{1}$$

Where denotes derivative concerning time, and with r_1 and r_2 as:

$$\begin{gathered} r_1 = \sqrt{(x-\mu)^2 + y^2 + z^2} \\ r_2 = \sqrt{(x-1+\mu)^2 + y^2 + z^2} \end{gathered} \tag{2}$$

The pseudo-potential function U is:

$$U = \frac{1}{2}(x^2 + y^2) + \frac{1-\mu}{r_1} + \frac{\mu}{r_2} \tag{3}$$

The CR3BP has a notable quantity called the Jacobi constant, denoted as JC. It is defined as JC = 2U - v^2, where v represents the magnitude of the spacecraft velocity in the rotating frame. The Jacobi constant is a parameter similar to energy and remains constant along a ballistic arc. It provides insights into the possible behavior of the system. For instance, a higher Jacobi constant implies a lower orbital energy, resulting in more restricted motion. In the six-dimensional phase space described by (1), a subset of invariant planar orbits exists, meaning their z-coordinate remains at zero. Additionally, there are several symmetries within the system. If (x(t), y(t), z(t)) is a solution to 1, then its reflection about the x-y plane, (x(t), y(t), -z(t)), is also a valid solution. Similarly, by reversing the direction of time, the reflection about the x-z plane is another valid solution, given by (x(-t), -y(-t), z(-t)). Furthermore, there is a symmetry concerning μ if (x(t), y(t), z(t)) is a solution for μ = μ_0 then (-x(-t), y(-t), z(-t))is a solution for $\mu = 1 - \mu_0$. There is then a symmetric axis in μ = 1/2.

A. *Libration points*

It is a widely acknowledged fact that for any given value of μ (where $0 < \mu < 1$), system 1 exhibits five equilibrium points in the orbital plane of the primaries (z = 0), as shown in figure 2. These points are commonly referred to as Lagrange[1] points or libration points. Among the libration points, three of them, named L1, L2, and L3, are positioned in a straight line with the primary bodies. L1 is situated between the two primaries, L2 is located beyond the smaller primary, and L3 is positioned beyond the larger primary. The remaining two libration points, L4 and L5, form an equilateral triangle with the primaries. Specifically, L4 can be found at coordinates (x, y) = (1/2 - μ, - $\sqrt{3/2}$), while L5 is located at (1/2 - μ, $\sqrt{3/2}$).It is important to note that as μ approaches 0, L1 and L2 merge together, and as μ approaches 1, L1 and L3 merge.Additionally, there is a symmetry relationship with respect to μ = 1/2. 2

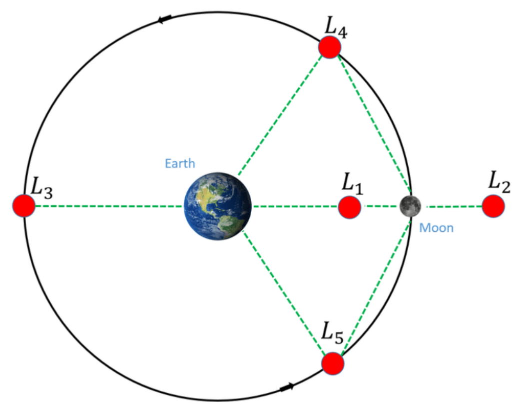

Fig. 2: Lagrange points on the CR3BP [7]

B. *Periodic Orbits*

When system 1 is expressed as a first-order system in R6, the Jacobian matrix evaluated at the libration points L1, L2, and L3 exhibits two pairs of purely imaginary eigenvalues. These eigenvalues are responsible for well-known families of periodic orbits, namely the planar Lyapunov orbits denoted as **L1**, **L2**, and **L3**, as well as the Vertical orbits denoted as **V1**, **V2**, and **V3**. Similarly, the Jacobian matrix at the libration points L4 and L5 always possesses at least one pair of purely imaginary eigenvalues for all values of μ. This gives rise to the families **V4** and **V5** of Vertical orbits originating from L4 and L5, respectively. For values of μ below a critical threshold μ_2, approximately equal to 0.0385, the Jacobian matrix at the libration points L4 and L5 exhibits an additional two pairs of purely imaginary eigenvalues. These additional eigenvalues generally lead to the emergence of two families of planar orbits for both L4 and L5. [8]

[1]Despite being all named Lagrange points, the collinear equilibrium points were found by Euler (1767) while the triangular equilibrium points were worked out by Lagrange (1772)

III. Orbital Stability and Bifurcations

Stability indices provide valuable information about the stability of an orbit. This metric is defined as

$$\nu = \frac{1}{2}(\lambda^{W_s} + \lambda^{W_u}) \tag{4}$$

where λ represents the eigenvalues of the monodromy matrix, $\phi(t+P,t)$, and P is the orbital period of the baseline orbit in the CR3BP. [9] It is worth noting that the eigenvalues of the monodromy matrix are observed as two sets of reciprocal pairs and two trivial eigenvalues with a value of unity, which arise from the periodic nature of the solution.

The nontrivial four eigenvalues consist of a pair associated with the stable/unstable subspace and another pair representing the center subspace. Since there is one stable and one unstable mode, the stability indices are calculated by taking the average of the (reciprocal) pair of multipliers related to the stable subspace ($|\lambda_s| < 1$) and the unstable subspace ($|\lambda_u| > 1$). These eigenvalues are also used to isolate intersections with other families of orbits in the solution space. In this study, all of the solutions examined possess six characteristic multipliers in reciprocal pairs.

When the characteristic multipliers λ_s and λ_u associated with the stable and unstable subspaces are equal to ±1, the reference trajectory represents the precise intersection between two distinct families of orbits. As a result, the orbit becomes a subset of both families, indicating a bifurcation point where the trajectory exhibits characteristics of both families simultaneously. Additionally, if the characteristic multipliers λ_c and λ_c^* corresponding to the center subspace are such that $\lambda_c = \lambda_c^*$ = ±1, the solution or orbit also defines the intersection point between two different families. In this case, when $\lambda_s = \lambda_u$ = ±1 and $\lambda_c = \lambda_c^*$ = ±1 occur simultaneously, the trajectory solution belongs to three distinct families of orbits. As a consequence, three families intersect at this point, leading to a phenomenon known as trifurcation.

When examining the Lyapunov families, the first two bifurcations occur when exploring the solution space for all three Lyapunov families. These bifurcations are specifically associated with the condition where the center multipliers, λ_c and λ_c*, are equal to ±1. Initially, the multipliers in the center subspace for all three families (**L1, L2, L3**) are distributed along the unit circle, which aligns with our expectations. However, as the solution space is expanded, these families exhibit bifurcations with the halo orbit families. During these bifurcations, the center multipliers transition to real values instead of remaining on the unit circle.

Apart from the previously mentioned bifurcation types, there are additional types of bifurcations that should be considered. Specifically, in the context of studying and applying Halo orbits, period-multiplying bifurcations play a significant role.

A. Period-multiplying bifurcations

Can occur without any changes in the orbital stability. For instance, when two nontrivial eigenvalues of the monodromy matrix, λ_c = -1, are present, a period-doubling bifurcation takes place. However, period-multiplying bifurcations (with a multiplying factor m) occur when two nontrivial eigenvalues of the monodromy matrix are expressed as $\lambda_c = \lambda_c^*$ = cos(2π/m) ± i*sin(2π/m). These period-multiplying bifurcations give rise to a set of new families of orbits originating from the NRHO family. These bifurcations provide an avenue for exploring and discovering new orbital configurations and behaviors within the HALO orbit family.

For period-multiplying bifurcations (and the resulting higher-period families) the naming format is defined: ‘Pm[originating family]n’, where ‘Pm’ refers to the order of the period-multiplication (e.g., period-doubling is reflected in m = 2), ‘[originating family]’ refers to the family from which the bifurcating family has evolved (e.g., ‘HO’ refers to halo orbits and ‘DRO’ refers to distant retrograde orbits), and ‘n’ denotes a sub-family identifier (i.e., for multiple bifurcations of the same type, the first family, in order of increasing perilune radius, is labelled n = 1, the second family is labelled n = 2, etc.).

Regarding the period-doubling bifurcations, two families emerge from the NRHO family: $P2HO_1$ and $P2HO_2$. With respect to the period-quadrupling bifurcations, another two families emerge: $P4HO_1$ and $P4HO_2$. The following sections of this paper will focus on the $P2HO_1$ family, commonly known as the Butterfly family [3]. Butterfly orbits have been of interest in space exploration and satellite missions for several reasons. They offer stable orbits that require relatively little propulsion or station-keeping maneuvers to maintain the spacecraft’s position. They also provide continuous visibility of both the larger bodies (such as the Earth and the Moon) and allow for extended observation or communication coverage. In figure 3 the Halo and Butterfly families are plotted together.

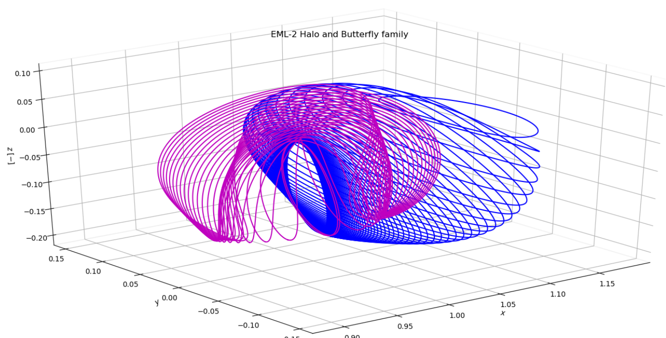

Fig. 3: Halo-Butterfly families transition

All the results presented in this work were carried out in SEMpy [10], a simulation environment for the circular restricted three-body problem, based on Python and developed by SaCLaB at ISAE-SUPAERO.

IV. Butterfly orbital family

Employing a multiple-shooting pseudo-arclength continuation scheme, the new families of periodic orbits originating at each of these bifurcations are computed. The Butterfly family originating from the NRHO bifurcation is plotted (and colored by Jacobi constant) in figure 4. Note that in figures 4 and 5 the southern orbits (or the segment of the family that possesses a majority of motion in the negative z-direction) are plotted (a northern analog also exists).

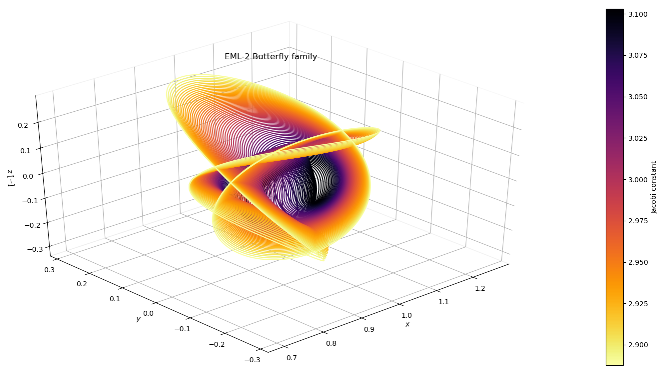

Fig. 4: 3D Butterfly Family

As can appreciated in figure 5, this family is characterized by two lobes in a “figure-8” shape, one on the L1 side of the Moon and one on the L2 side each having 5 to 7 day period ranges. [11] A distinct advantage for periodic orbits in this family is the ability to access both sides of the Moon using natural ballistic motion.

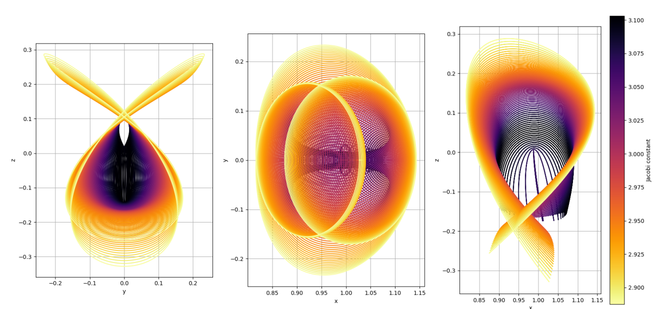

Fig. 5: Butterfly Family 2D projections

A. *Stability and Jacabi constant properties*

The behavior of the butterfly family undergoes intricate changes in terms of its geometry, period, energy, and stability properties. The analysis of its stability evolution employs a different approach to the stability index compared to the one presented in Section III.

This study utilizes an alternative formulation of the stability index to capture the full implications of complex eigenvalues deviating from the unit circle. Referred to as ζ, it is defined as:

$$\zeta = \frac{1}{2}(||\lambda_i|| + ||\lambda_i||^{-1}) \tag{5}$$

for $i = 1, 2$. This alternative stability index is a real value with a magnitude greater than or equal to 1^2.

[2]This alternative formulation sacrifices certain details, such as the sign of the eigenvalues.

Figure 6 displays the alternative stability indices, ζ, for a significant portion of the butterfly family. As a result, the range of orbits depicted in the stability index plot is significantly broader than the range of orbits presented in the visualization of the halo-butterfly bifurcation in figure 3. The extended coverage of the butterfly family reveals numerous stability transitions throughout its evolution.

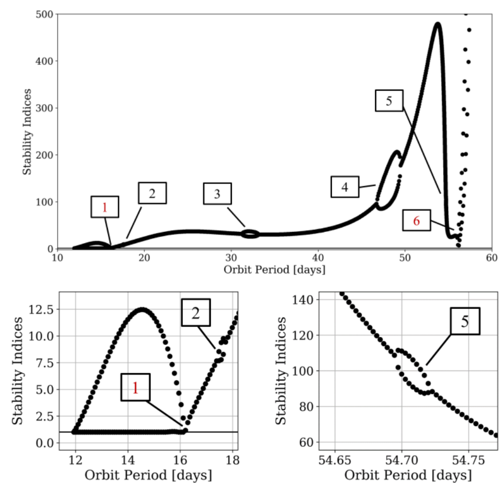

Fig. 6: Alternative orbital stability evolution [12]

Figure 6 illustrates the diverse eigenstructures present in the butterfly family. These eigenstructures have significant implications for mission design. The range of butterfly orbits analyzed so far exhibits a variety of eigenstructures and stability properties, which directly impact the available manifold structures. This is particularly relevant when considering low-cost transfers. Additionally, the magnitude of the stability indices is correlated with station-keeping and transfer costs, with smaller stability indices typically resulting in lower station-keeping costs [12].

The evolution of the Jacobi constant value, denoted as C, for the butterfly family exhibits a less complex behavior compared to its stability evolution. Figure 7 displays the evolution of the Jacobi constant value for the butterfly family and the 9:2 NRHO orbit. It is evident that within this range of the butterfly family, only one orbit shares the same Jacobi constant value as the 9:2 NRHO orbit, suggesting a potential no-cost transfer possibility at that specific point.

For the family's remaining orbits, the Jacobi constant value change is relatively small during the initial portion of the curve. However, there is a noticeable drop in the Jacobi constant value at an orbit period of approximately 50 days. In general, the smaller the difference in Jacobi constant value between two orbits, the lower the transfer cost. As a result, butterfly orbits with lower Jacobi constant values (corresponding to higher energy levels) tend to have relatively higher transfer costs.

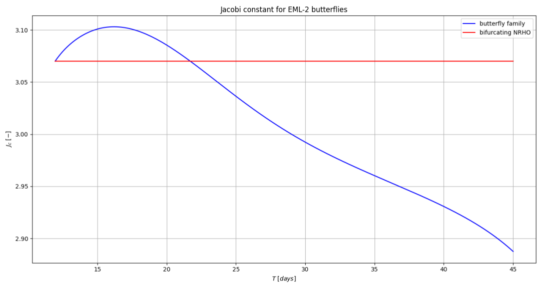

Fig. 7: Jacobi constant evolution

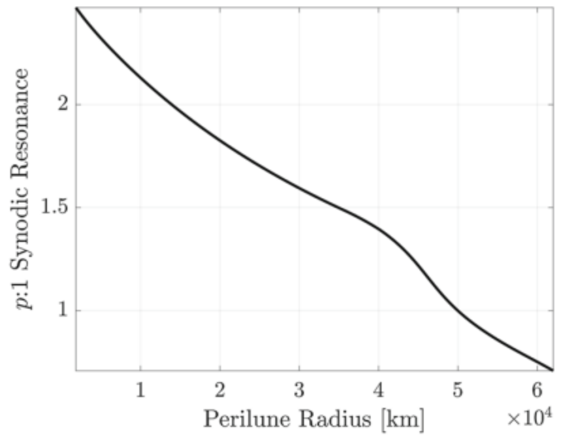

Fig. 8: p=1 synodic resonances in Butterfly orbits [2]

B. Resonance properties

Resonance in terms of the synodic period is defined as the time between successive conjunctions of a celestial body with the Sun, i.e., the time required for the Earth–Moon–Sun orientation to repeat. In this case, a viewer fixed at the center of the Earth would see the Moon return to the same location with respect to the Sun after one synodic period of the Moon, however, the Moon would not appear in the same location to an observer in an inertial frame fixed at the center of the Earth. The Moon's synodic period is approximately 29.5 days, slightly longer than its sidereal period (approximately 27.3 days). The synodic period is also denoted as a lunar month since the full lunar cycle (i.e., time between successive full Moon phases) requires one synodic period to complete.

Orbital resonance is defined in terms of a p:q ratio, where p indicates the number of completed revolutions of a given periodic orbit over q synodic periods of the Moon. The value of p divided by q must be positive and rational, i.e., both p and q can be written as positive integers. As an example of orbital resonance, a 4:1 synodic resonant NRHO possesses a period of approximately 7.375 days such that four revolutions of the spacecraft in this orbit can be completed over the duration of one synodic period of the Moon (7.375 days * 4 = 29.5 days). [2]

1) Eclipse avoidance in the Butterfly orbits:

Eclipse avoidance in space missions is a crucial consideration for space missions, especially those involving spacecraft that rely on solar power. It helps maintain power supply, thermal stability, data continuity, operational stability, and battery conservation, thereby enabling the success and longevity of spacecraft operations.

Specific resonant solutions from the $P2HO_1$ family will be investigated further due to their favorable long-duration eclipse avoidance properties. In figure 8, it is apparent that 2:1, 1:1, and 3:2 (equivalently, 3/2:1) synodic resonant orbits exist across the region of the $P2HO_1$ family.

The 2:1 synodic resonant $P2HO_1$ orbit is illustrated in figure 9 in Earth-Moon synodic reference frame. In the CR3BP, this butterfly orbit is defined with a perilune radius of 13967 km and an orbital period of 14.76 days. It is the most stable of the three orbits but still unstable. The maximum stability index is $\nu = 12.31$ (corresponding to a time constant of $\tau = 0.0919$ revolutions); unstable orbits potentially possess useful manifold structures for transfer design.

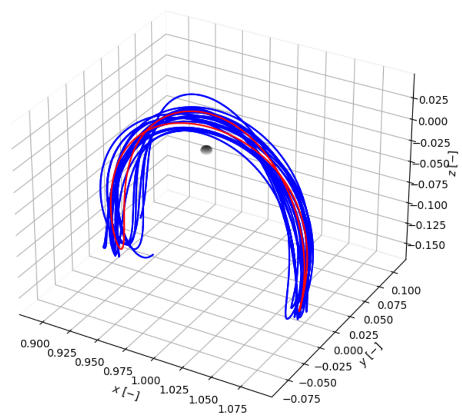

Fig. 9: Butterfly 2:1 ephemeris model

In figure 9, the red orbit corresponds to the solution in the CR3BP, while the blue trajectory corresponds to 15 revolutions (221.3 days) of the orbit computed in the higher-fidelity ephemeris [3] model.

[3]The ephemeris model takes into account the gravitational interactions among celestial bodies, such as the Sun, planets, and moons, and factors in other influences like perturbations from other bodies, relativistic effects, and more. By considering these various forces, the model can calculate celestial objects' precise positions and velocities at a given time.

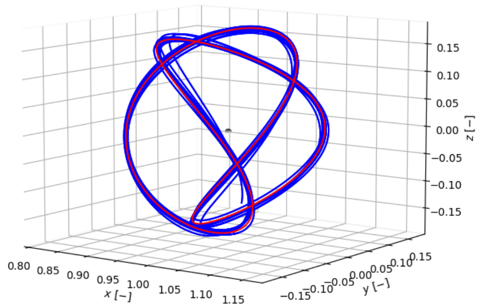

Fig. 10: Butterfly 1:1 ephemeris model

Figure 10 illustrates the representation of the 1:1 synodic resonant $P2HO_1$ orbit in Earth-Moon rotating frame. The orbit's perilune radius is measured at 49986 km, and in the context of the Circular Restricted Three-Body Problem (CR3BP), its period corresponds to the synodic period of the Moon, which is approximately 29.5 days.

Regarding the stability index, it is the most unstable with $\nu = 33.55$ or time constant of $\tau = 0.03499$ revolutions. The orbit exhibits both unstable and stable spiral manifold structures, which have the potential to be useful in transfer design within the specific region.

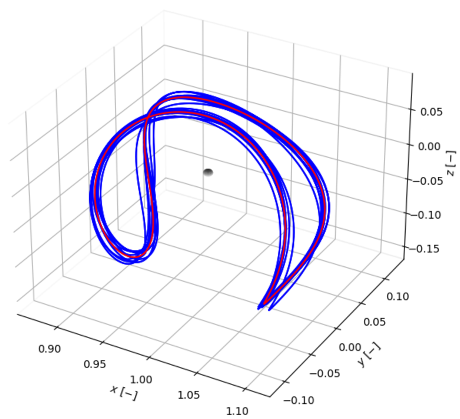

Fig. 11: Butterfly 3:2 ephemeris model

Figure 11 depicts the 3:2 synodic resonant P2HO1 orbit. In the context of the CR3BP, this periodic solution has a perilune radius of 34970 km and a period of 19.67 days. A calculated ephemeris solution covering a duration of 295 days successfully avoids both lunar and Earth eclipses.

The maximum stability index is $\nu = 19.94$, indicating its overall stability. Alternatively, the associated time constant for this orbit is $\tau = 0.05988$ revolutions. Notably, this specific P2HO1 orbit exhibits both stable and unstable spiral manifold structures, which hold the potential for facilitating transfer design either into or out of the vicinity of the orbit.

To determine whether the three orbits avoid solar and lunar eclipses, they need to be observed in the Sun-Earth and Sun-Moon synodic reference systems. By examining the paths of the shadow of the Earth and the Moon, it can be determined whether or not these orbits intersect with the shadow regions.

If an orbit does not intersect with the shadow of the Earth or the Moon, it can be considered to avoid solar and lunar eclipses. Conversely, if the orbit passes through or intersects with these shadow regions, it may be subject to solar and lunar eclipses during its trajectory.

- **Sun-Earth reference frame:** To transform an orbit from the Earth-Moon synodic reference frame to the Sun-Earth synodic reference frame, the following steps can be taken:
  1) Transformation to the Earth-Centered Inertial (ECI) system:
     - Use the appropriate rotation matrix that corresponds to the dimensionless time of each position and velocity vector. Apply this rotation matrix to convert each vector from the Earth-Moon synodic reference frame to the ECI system.
     - Subtract the displacement of the center μ from the $x_{inertial}$ coordinate. This accounts for the fact that the center is displaced from the center of the Earth in the ECI system.
  2) Transformation from the ECI system to the Sun-Earth synodic reference frame:
     - In this transformation, the dimensional units need to be adjusted to match the Sun-Earth system.
     - Multiply each time value by the ratio of the synodic periods or the ratio of the orbital periods in the two systems.
     - Scale the position vector by the ratio of the characteristic lengths in the two systems.
     - Scale the velocity vector by the ratio of the length to the ratio of the time units.
     - Use the inverse of the rotation matrix that was used in the first transformation. Apply this inverse rotation matrix to convert the position and velocity vectors from the ECI system to the Sun-Earth synodic reference frame.

By following these steps, the orbit can be successfully transformed from the Earth-Moon synodic reference frame to the Sun-Earth synodic reference frame, accounting for the rotation matrices, dimensional unit conversions, and displacement of the center.
Figures 12, 13, and 14 depict the transformed orbits in the Sun-Earth synodic reference frame. It is evident from these figures, particularly from the z-y projections, that the three orbits successfully avoid sun eclipses. The visualization clearly shows that the orbit paths never intersect with the Earth's shadow (it would be projected along the x axis), indicating that there is no interference between the orbits and the Earth during their respective trajectories.

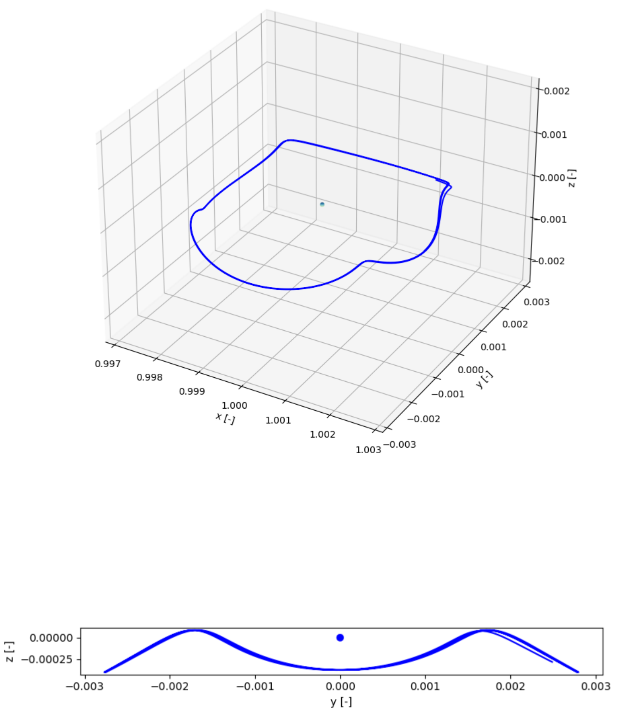

Fig. 12: Butterfly 2:1 Sun-Earth Synodic reference frame

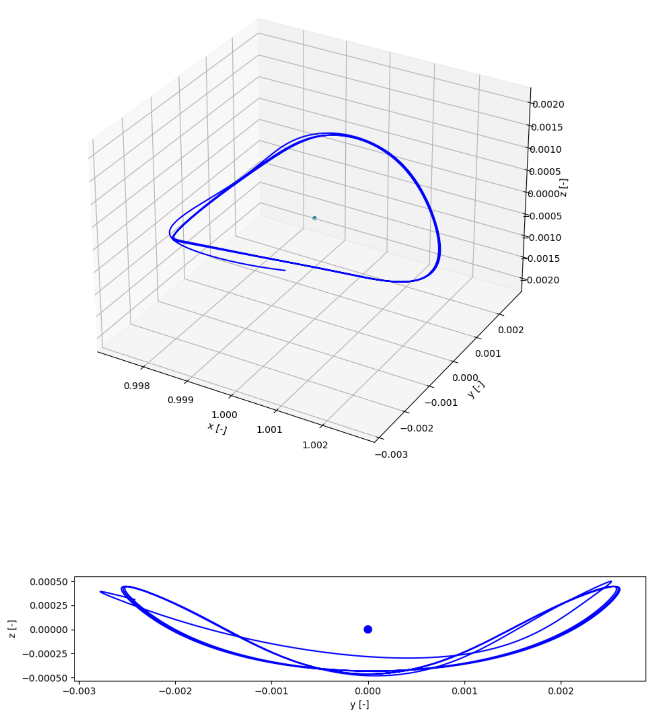

Fig. 13: Butterfly 1:1 Sun-Earth Synodic reference frame

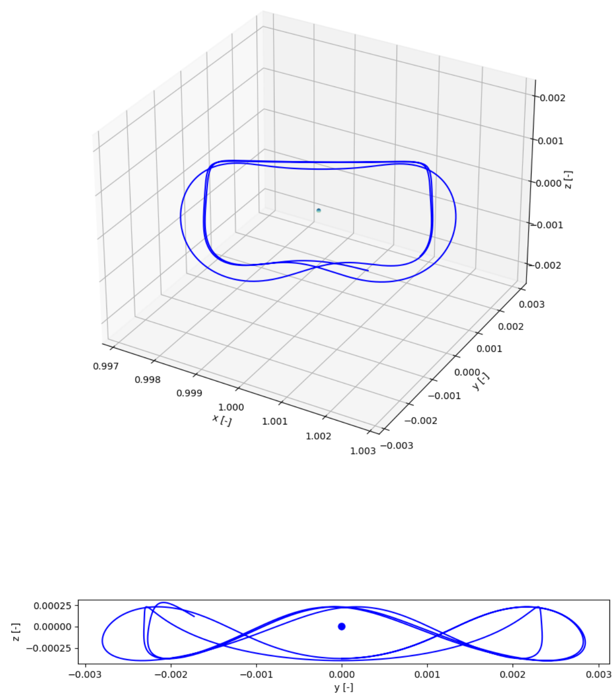

Fig. 14: Butterfly 3:2 Sun-Earth Synodic reference frame

- **Sun-Moon reference frame:** To transform an orbit from the Earth-Moon synodic reference frame to the Sun-Moon synodic reference frame, the following steps can be taken:
  1) Transformation to the Moon-Centered Inertial (MCI) system:
     Following the same procedure that the one to convert to the ECI, the corresponding rotation matrix will be apply to convert each vector to the MCI system.
     Then, unlike with the ECI system, the value $1-\mu$ will be add to the $x_{inertial}$ coordinate. Being displaced the center to the center of the MCI system.
  2) Transformation from the MCI system to the Sun-Moon synodic reference frame:
     – In this transformation, the dimensional units need to be adjusted to match the Sun-Moon system.
     – Multiply each time value by the ratio of the synodic periods or the ratio of the orbital periods in the two systems.
     – Scale the position vector by the ratio of the major axis of the second body in the two systems. In this case, this value is equal to 1, due to the second body is the same (Moon) for both reference frames.
     – Scale the velocity vector by the ratio of the length to the ratio of the time units.
     – Use the inverse of the rotation matrix that was used in the first transformation. Apply this inverse rotation matrix to convert the position and velocity vectors from the MCI system to the Sun-Moon synodic reference frame.

By following the aforementioned steps, the orbit can be effectively converted from the Earth-Moon synodic reference frame to the Sun-Moon synodic reference frame, taking into account the rotation matrices, dimensional unit conversions, and displacement of the center.
Figures 15, 18, and 20 illustrate the transformed orbits in the Sun-Moon synodic reference frame. The 2D visualizations clearly demonstrate that all three orbits successfully avoid solar eclipses, as the paths of the orbits do not intersect with the Moon's shadow. This observation holds significant importance, as the avoidance of solar eclipses is essential for the safe and efficient operation of space missions.

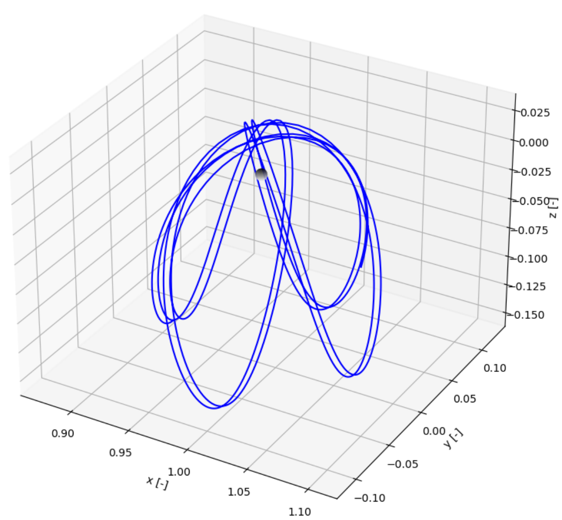

Fig. 15: Butterfly 2:1 Sun-Moon Synodic reference frame

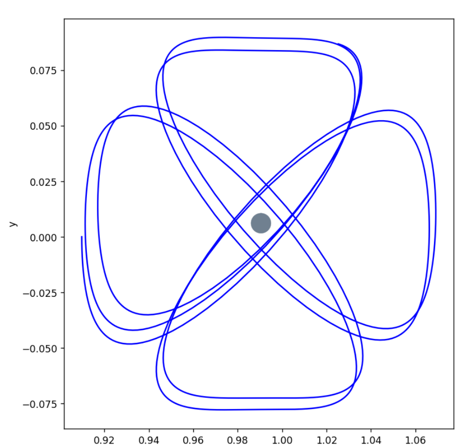

Fig. 16: Butterfly 2:1 Sun-Moon Synodic reference frame xy projection

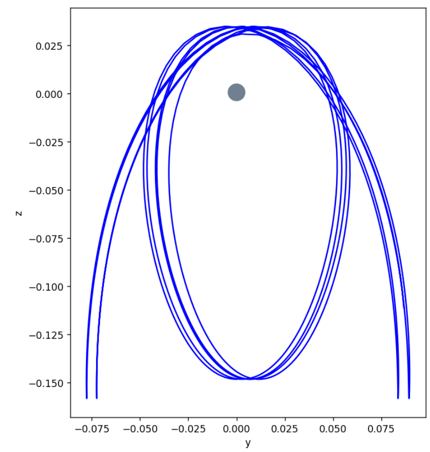

Fig. 17: Butterfly 2:1 Sun-Moon Synodic reference frame yz projection

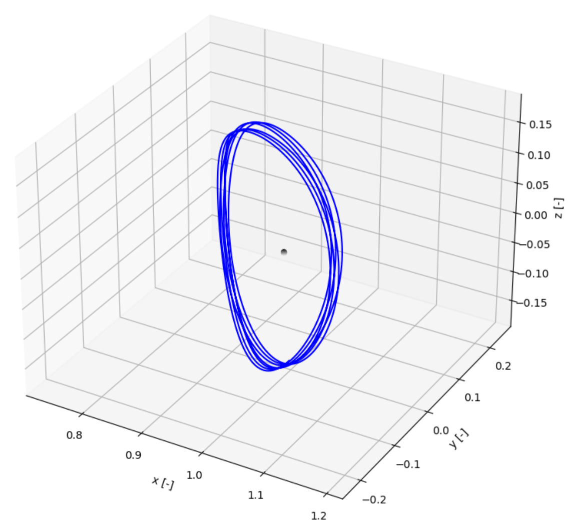

Fig. 18: Butterfly 1:1 Sun-Moon Synodic reference frame

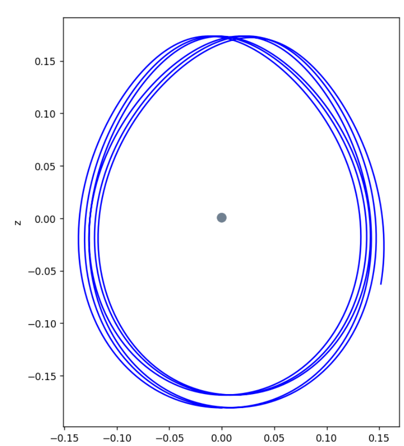

Fig. 19: Butterfly 1:1 Sun-Moon Synodic reference frame yz projection

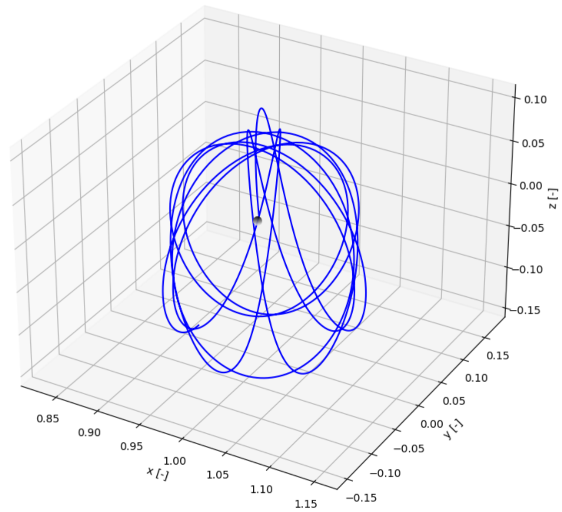

Fig. 20: Butterfly 3:2 Sun-Moon Synodic reference frame

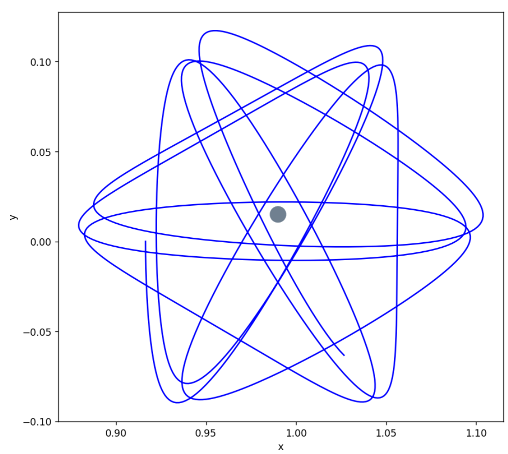

Fig. 21: Butterfly 3:2 Sun-Moon Synodic reference frame xy projection

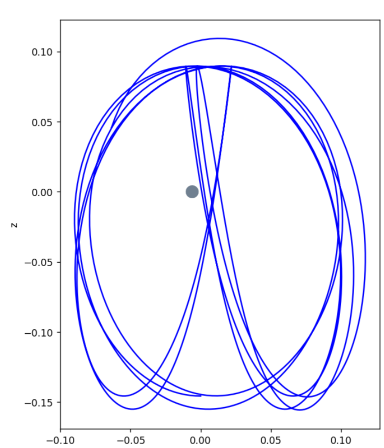

Fig. 22: Butterfly 3:2 Sun-Moon Synodic reference frame yz projection

C. Lunar coverage and station-keeping cost

There has been significant interest in exploring and investigating the lunar south pole in recent years, primarily due to its potential for harboring frozen volatiles [4]. [13] This region has distinct scientific and strategic advantages, making it an attractive target for space exploration missions. A key aspect of lunar south pole coverage involves using two satellites, and within the context of the three-body problem, there may be viable architectures for achieving this. [14]

The selection of orbits plays a crucial role in determining lunar south pole coverage. Two criteria are considered: the time required to complete one full period and the feasibility of achieving coverage. Once a specific architecture is chosen, the orbit is discretized into a series of patch points. Using a corrections scheme proposed by Wilson and Howell [15], these patch points are then adjusted to meet the desired time-of-flight and orbit periodicity requirements.

Considering the long-term station-keeping costs is also crucial in assessing the feasibility of these systems. Minimizing costs is advantageous in this regard. The study by D.J. Gregow et al. [14] analyses the lunar coverage and station-keeping cost of two satellites in the same or different orbits. The butterfly family of orbits, characterized by a specific time to complete one full period and feasibility for lunar south pole coverage, is selected for further analysis. The HALO family is also selected for analysis. A combination between the 14-day L_2 butterfly orbit and the 7-day L_2 HALO orbit is realized, obtaining a region of dual coverage of 50º- While taking into account only the 14-day butterfly orbit, the region of dual coverage is 45º. [5]

From that same study, the data shown in the table I are presented:

Orbit type	Period days	Stability index	Total ΔV [m/s]
NRHO L2	7.0	1	4.82
NRHO L1	8.0	1.25	5.54
HALO L1	12.0	60	66.33
Vertical L1	14.0	690	171.82
Butterfly L2	14.0	11.3	31.86

TABLE I: Station keeping result for one year [14]

A clear relationship between the stability index and the station-keeping cost can be observed upon qualitative analysis of the results. Orbits with higher stability indices, indicating less stability, tend to require more fuel for station-keeping compared to orbits with lower stability indices. This can be exemplified by the vertical orbit, which exhibits a higher stability index and thus would necessitate a greater amount of fuel for maintaining its desired trajectory.

Additionally, it is interesting to note that despite the butterfly orbit having a total period of 14 days, it exhibits a distinctive pattern with two lobes, each situated on one side of the moon. This configuration effectively creates a periodicity of

[4] Substances that have frozen or solidified due to extremely low temperatures in certain regions of the lunar surface. These volatiles include compounds such as water ice, carbon dioxide (CO_2), methane (CH_4), and other volatile compounds.

[5] At least one spacecraft is always 45º above the horizon

approximately 7 days, which can be considered when planning and scheduling mission operations.

These qualitative observations highlight the importance of stability and periodicity in orbital dynamics, as they directly impact the operational costs and feasibility of maintaining desired orbits for space missions.

Finally, the study identifies the butterfly family as a solution to the challenges associated with lunar south pole coverage, having good coverage and an affordable station-keeping cost (thanks to their stability properties).

V. Transfer to butterfly orbits

In this section, an analysis of transfer costs [6] associated with Earth to Moon transfers for the lunar mission will be made. Understanding these costs is crucial in selecting the optimal target orbit for the mission. Various factors influence the transfer costs, and by considering them, informed decisions can be made to minimise energy requirements and maximise mission efficiency.

In order to carry out this analysis, two main factors have been taken into account:

- **ΔV Requirements:** ΔV, or change in velocity, is a key parameter that determines the energy needed for a spacecraft to transition from Earth's orbit to the Moon's orbit. It encompasses both the departure from Earth's orbit and the arrival at the Moon's orbit. Analyzing the delta-V requirements for different transfer trajectories allows us to assess the fuel consumption and propulsion system capabilities needed for the mission.
- **Trajectory Optimization:** Trajectory Optimization: The path taken by the spacecraft during the transfer can be optimized to minimize energy consumption. This involves careful analysis of various trajectory options, such as direct transfers or complex multi-impulse trajectories. Considering factors such as duration, fuel consumption, and arrival-departure points, advanced optimization algorithms will be employed to search for the most efficient trajectory within the given constraints, for different kind of missions.

By studying and quantifying these transfer costs, the overall feasibility and efficiency of different target orbits for the lunar mission can be assessed. At the end of this analysis, it will be possible to compare the mission requirements for various Butterfly and NRHO orbits, as was done for station-keeping costs in Section IV.

To compute the transfer from a geocentric orbit to a lunar orbit, the following steps can be taken:

1) **Computation of an Earth parking orbit**
First of all, our desired orbit's characteristics must be chosen. In this research, the parking orbit will be initialised through the desired Keplerian elements. In the case concerning this paper, the parking orbit used to calculate the transfer costs, is a circular[7] LEO orbit with a height of 500km over the Earth's surface (it's remaining Keplerian elements are i = 0º, $\Omega = 125.08$º, $\omega = 318.15$º, and $\nu = 139.87$º). Once the orbit's elements have been chosen, translation to the Cartesian coordinates system by using the function ”keplerian-to-cartesian-elementwise” from the tudatpy module must be done before propagating them on the J2000 reference frame [8], by the use of a numerical simulator. In order to have useful results from the propagation, the time and state vectors from the simulation will be extracted.

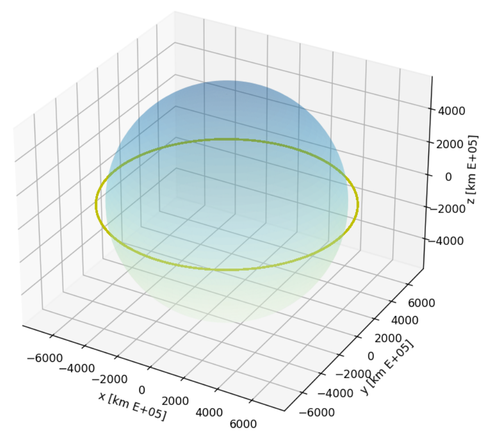

Fig. 23: Earth's parking orbit in the J2000 Frame

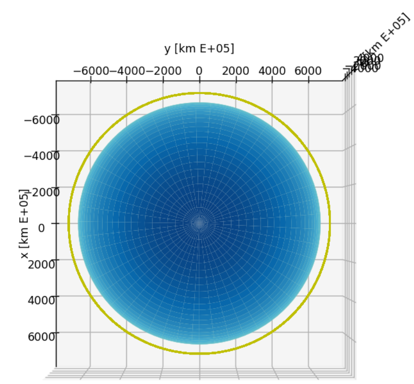

Fig. 24: Earth's parking orbit in the J2000 Frame seen from the zenith

2) **Transformation from the Earth's J2000 frame to the Earth-Moon Synodic frame**
Since SEMpy has been used for this study, the time and state vectors of the J2000 reference frame will have to be translated into the Earth-Moon synodic frame. In contemplation of this goal, use of the ”j2000-to-synodic”

[6]The transfer costs studied in this section are direct transfer costs based on the Lambert Transfer, for better results, the use of manifold structures should be taken into account.

[7]Circular orbit implies e=0.

[8]The J2000 (aka EME2000) frame definition is based on the earth's equator and equinox, determined from observations of planetary motions, plus other data. The name “J2000” is also used to refer to the zero epoch of the ephemeris time system (ET, also known as TDB). [16]

function will be taken, obtaining the parking orbit's time and state vectors in the desired frame.

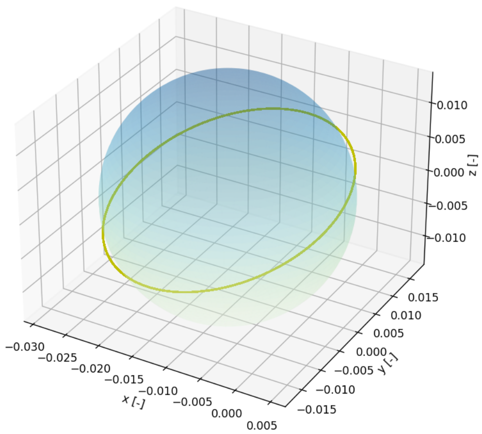

Fig. 25: Earth's parking orbit in the Earth-Moon Synodic Frame

3) **Computation of the target lunar orbit**
The computation of the target lunar orbit will be carried out in the CR3BP model, as will the Lambert's transfer in the next step. This solution will be obtained with the same method as have been previously done in this paper, via the interpolation of the orbit given the desired orbital period. As studied throughout the article, the three resonant butterfly orbits studied above will be computed, in addition to a 4:1 synodic resonant NRHO, with the purpose of comparing the direct transfer costs from Earth to both families.
4) **Computation of the Lambert Transfer**
Once computed the departure and arrival orbits, with their respective dimensionless state and time vectors, to perform the direct transfer, the Lambert problem for one revolution must be solved, taking use of the class "Cr3bpLambertPbm" from SEMpy. To obtain the solution to this problem, the departure point of the transfer (state of the parking orbit), the arrival point (state of the corresponding lunar orbit) and the time of flight (TOF) will have to be chosen, among other parameters.
By definition, the Lambert transfer seeks an orbit arc in the two-body problem that connects two points in space guaranteeing continuity of velocity and position. By using this method in this study, only an approximated value of the desired transfer cost between the Earth's parking orbit and the lunar orbit in question can be given, since at small changes in the time of flight, or in the departure and arrival positions and velocities, large difference in the ΔV values will be obtained as a solution to the problem.
5) **Optimization of the computed transfer trajectory**
Although the study carried out in this section is qualitative, for the reasons previously discussed, the obtained results can be optimized in a rather rudimentary way by choosing the departure and arrival points so that at the departure the velocity vector is as tangent as possible to the trajectory to be followed, and at the arrival, points with velocities in the same direction or the same plane. In this way, a better result can be obtained when choosing as arrival points the periapsis of the butterfly orbits whose velocity is tangent to the Lambert's transfer trajectory.
To further refine the optimisation results, use will be made of the "Trajectory" class [17], which employs the Primer Vector theory to assess optimality and provide a criterion to decrease the transfer cost by inserting intermediate impulsive manoeuvres along the trajectory.

A. *Comparison of Earth-to-lunar orbit transfer costs*

In the following, the results obtained by using the procedure previously described in the section will be shown. Differentiation will be made between four different transfers, with the previously described parking orbit being the departure orbit used at all times, varying the arrival orbit. In addition, the best results obtained for times of flight (TOF) of 4, 7, 10 and 12 days will be shown, differentiating the transfer to three types of arrival points (lunar periapsis with velocity in favour, with velocity against and one of the four states contained in the ecliptic plane), for a better analysis of the data. Despite only showing the best result obtained, more than two hundred trajectories have been simulated, these data can be consulted in Appendix A.

Time of Flight [days]	Arrival point	Number of impulses	Total ΔV [m/s]
4	Periapsis	3	4812
7	Periapsis	3	4700
10	Periapsis	3	4578
12	Periapsis	3	4630

TABLE II: Transfer costs from parking orbit to Butterfly 1:1

Time of Flight [days]	Arrival point	Number of impulses	Total ΔV [m/s]
4	Periapsis	3	5031
7	Ecliptic plane	4	5013
10	Periapsis	3	4708
12	Periapsis	3	4705

TABLE III: Transfer costs from parking orbit to Butterfly 3:2

Time of Flight [days]	Arrival point	Number of impulses	Total ΔV [m/s]
4	Periapsis	3	5041
7	Ecliptic plane	4	5090
10	Ecliptic plane	4	4964
12	Ecliptic plane	4	4824

TABLE IV: Transfer costs from parking orbit to Butterfly 2:1

Time of Flight [days]	Arrival point	Number of impulses	Total ΔV [m/s]
4	Periapsis	3	5084
7	Apoapsis	3	5265
10	Periapsis	3	4908
12	Apoapsis	3	4545

TABLE V: Transfer costs from parking orbit to NRHO 4:1

B. Comparison of Earth-to-lunar orbit transfer trajectories

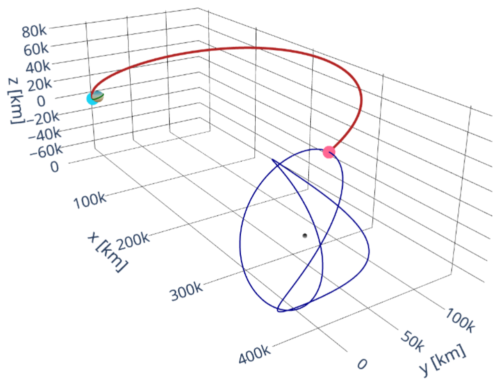

Fig. 26: Transfer trajectory to Butterfly 1:1 for TOF = 4 days and 2 impulses

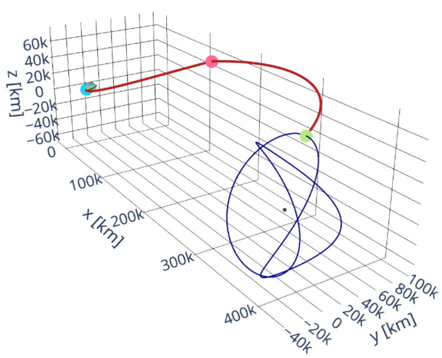

Fig. 27: Transfer trajectory to Butterfly 1:1 for TOF = 4 days and 3 impulses

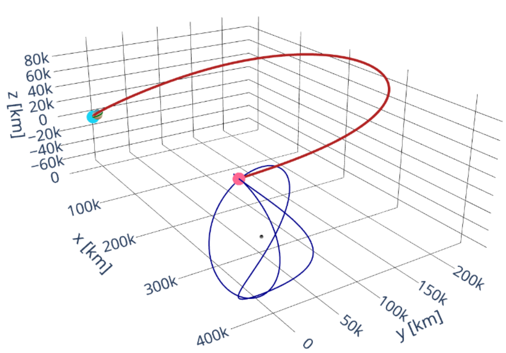

Fig. 28: Transfer trajectory to Butterfly 1:1 for TOF = 7 days and 2 impulses

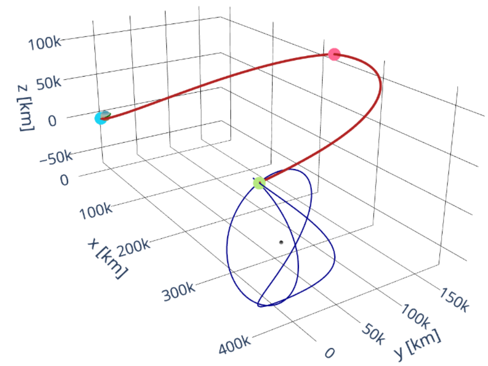

Fig. 29: Transfer trajectory to Butterfly 1:1 for TOF = 7 days and 3 impulses

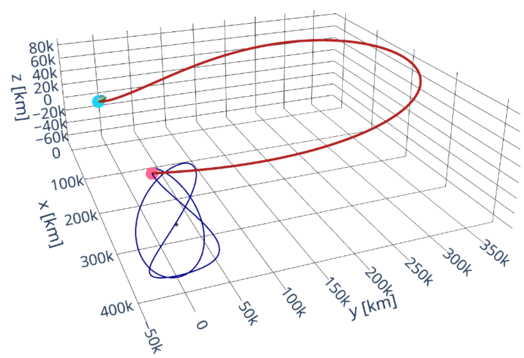

Fig. 30: Transfer trajectory to Butterfly 1:1 for TOF = 10 days and 2 impulses

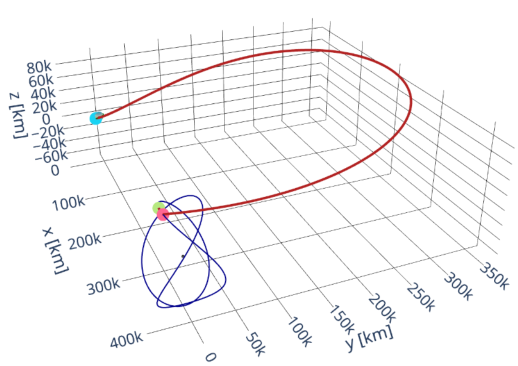

Fig. 31: Transfer trajectory to Butterfly 1:1 for TOF = 10 days and 3 impulses

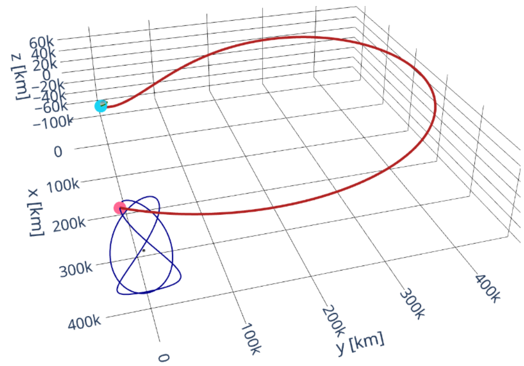

Fig. 32: Transfer trajectory to Butterfly 1:1 for TOF = 12 days and 2 impulses

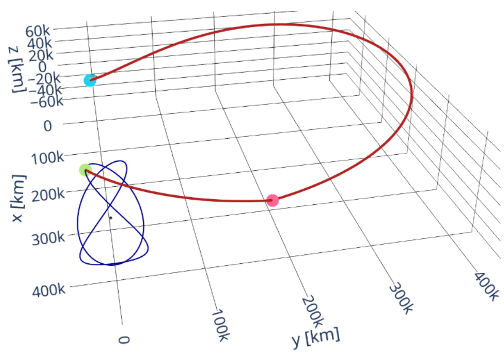

Fig. 33: Transfer trajectory to Butterfly 1:1 for TOF = 12 days and 3 impulses

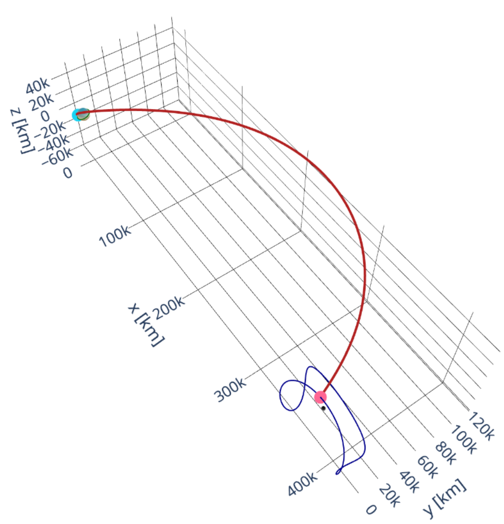

Fig. 34: Transfer trajectory to Butterfly 3:2 for TOF = 4 days and 2 impulses

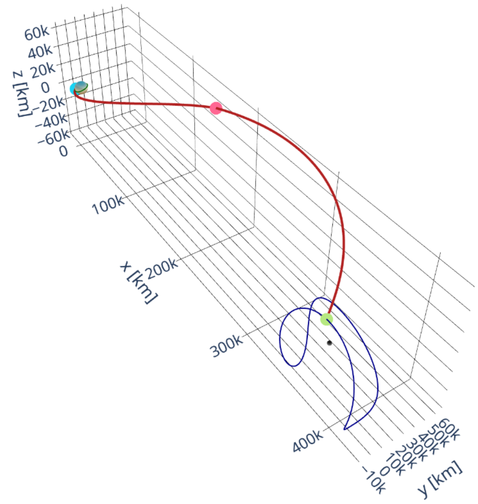

Fig. 35: Transfer trajectory to Butterfly 3:2 for TOF = 4 days and 3 impulses

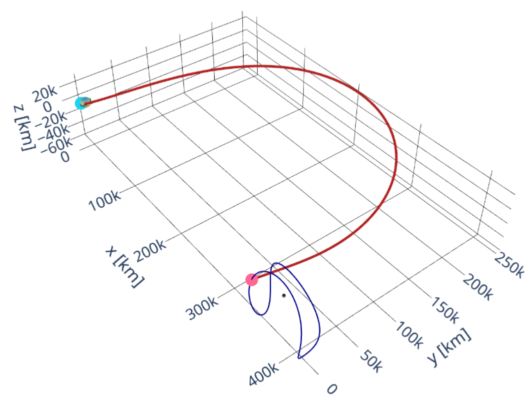

Fig. 36: Transfer trajectory to Butterfly 3:2 for TOF = 7 days and 2 impulses

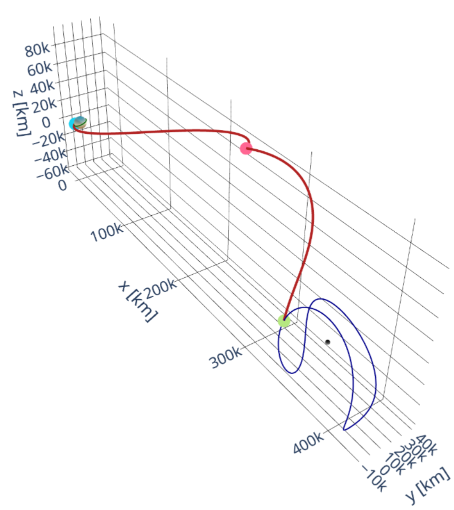

Fig. 37: Transfer trajectory to Butterfly 3:2 for TOF = 7 days and 3 impulses

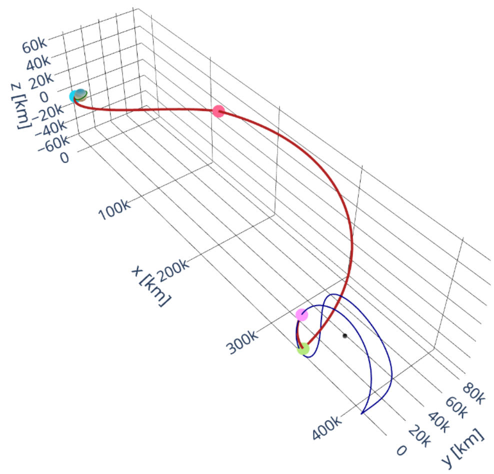

Fig. 38: Transfer trajectory to Butterfly 3:2 for TOF = 7 days and 4 impulses

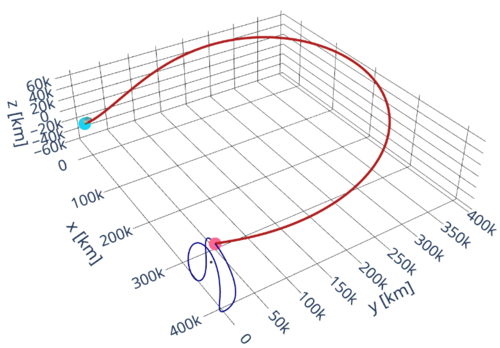

Fig. 39: Transfer trajectory to Butterfly 3:2 for TOF = 10 days and 2 impulses

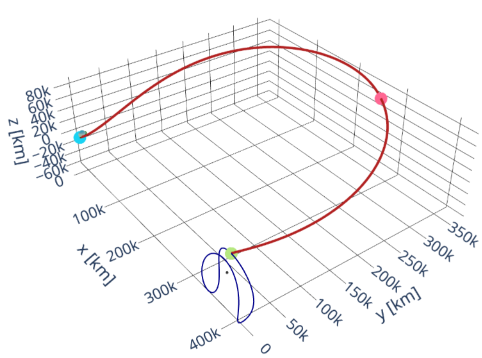

Fig. 40: Transfer trajectory to Butterfly 3:2 for TOF = 10 days and 3 impulses

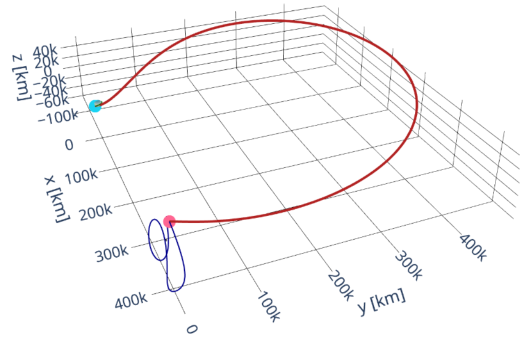

Fig. 41: Transfer trajectory to Butterfly 3:2 for TOF = 12 days and 2 impulses

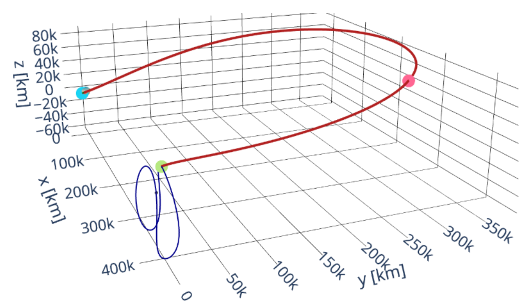

Fig. 42: Transfer trajectory to Butterfly 3:2 for TOF = 12 days and 3 impulses

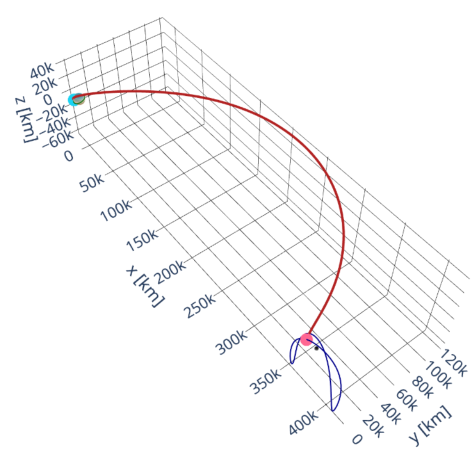

Fig. 43: Transfer trajectory to Butterfly 2:1 for TOF = 4 days and 2 impulses

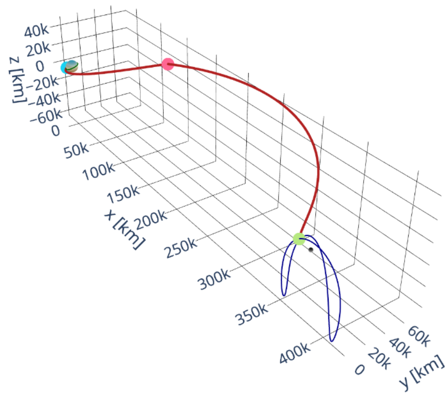

Fig. 44: Transfer trajectory to Butterfly 2:1 for TOF = 4 days and 3 impulses

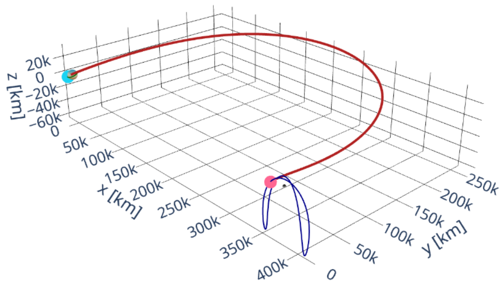

Fig. 45: Transfer trajectory to Butterfly 2:1 for TOF = 7 days and 2 impulses

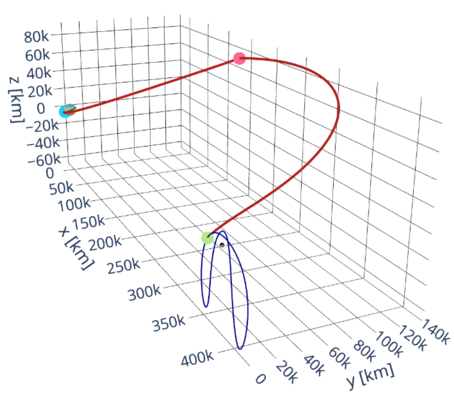

Fig. 46: Transfer trajectory to Butterfly 2:1 for TOF = 7 days and 3 impulses

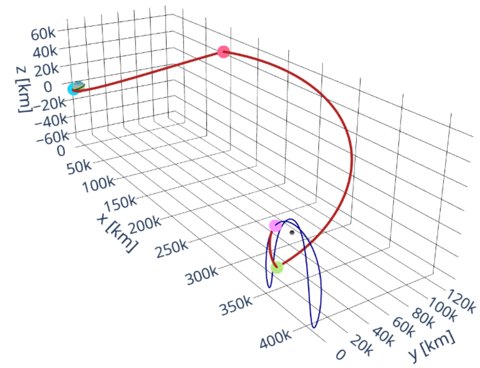

Fig. 47: Transfer trajectory to Butterfly 2:1 for TOF = 7 days and 4 impulses

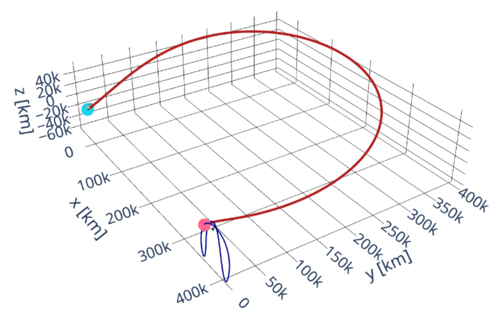

Fig. 48: Transfer trajectory to Butterfly 2:1 for TOF = 10 days and 2 impulses

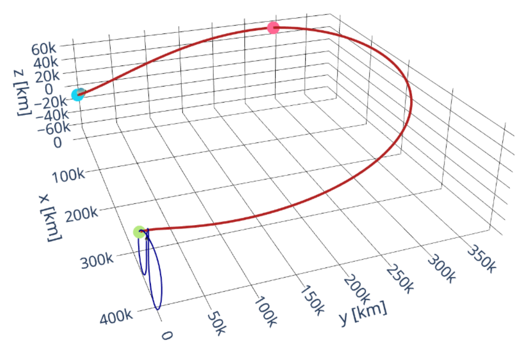

Fig. 49: Transfer trajectory to Butterfly 2:1 for TOF = 10 days and 3 impulses

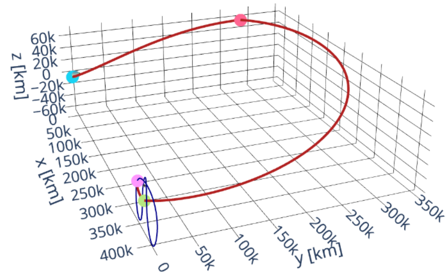

Fig. 50: Transfer trajectory to Butterfly 2:1 for TOF = 10 days and 4 impulses

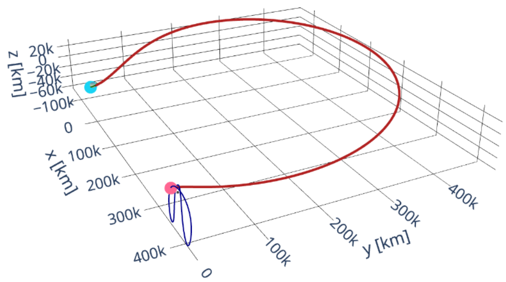

Fig. 51: Transfer trajectory to Butterfly 2:1 for TOF = 12 days and 2 impulses

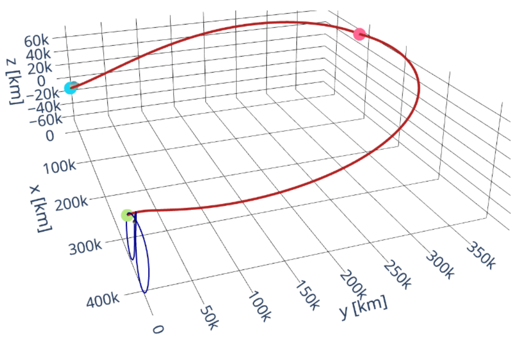

Fig. 52: Transfer trajectory to Butterfly 2:1 for TOF = 12 days and 3 impulses

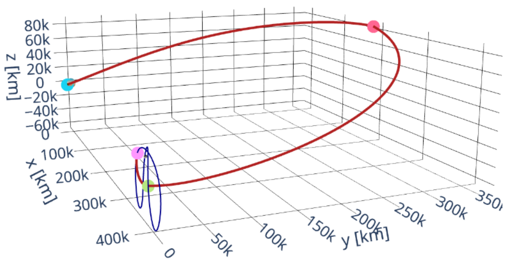

Fig. 53: Transfer trajectory to Butterfly 2:1 for TOF = 12 days and 4 impulses

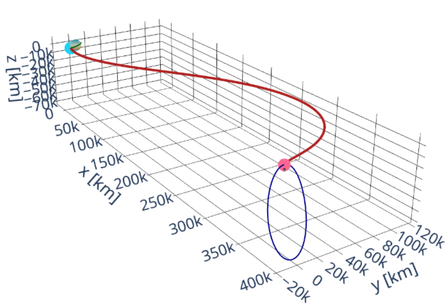

Fig. 54: Transfer trajectory to NRHO 4:1 for TOF = 4 days and 2 impulses

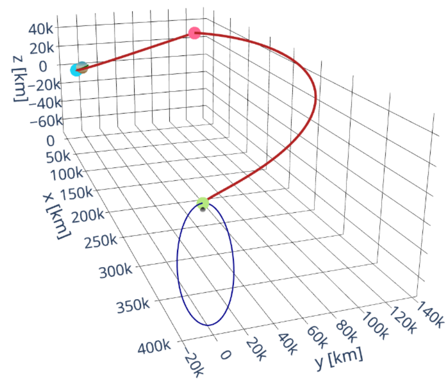

Fig. 55: Transfer trajectory to NRHO 4:1 for TOF = 4 days and 3 impulses

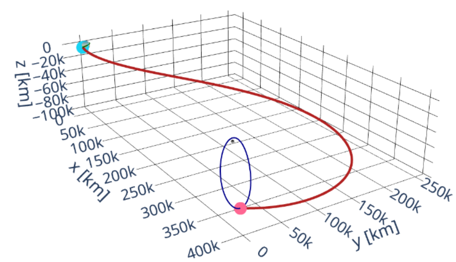

Fig. 56: Transfer trajectory to NRHO 4:1 for TOF = 7 days and 2 impulses

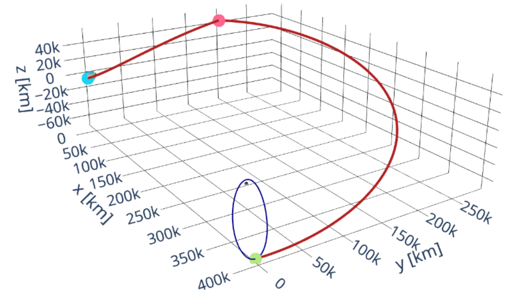

Fig. 57: Transfer trajectory to NRHO 4:1 for TOF = 7 days and 3 impulses

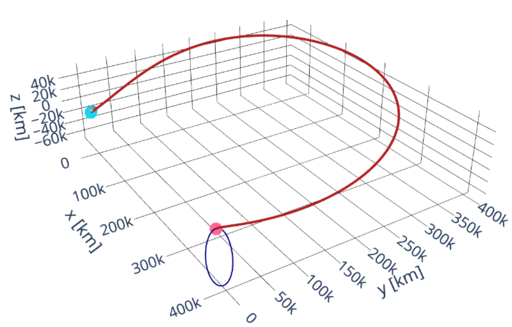

Fig. 58: Transfer trajectory to NRHO 4:1 for TOF = 10 days and 2 impulses

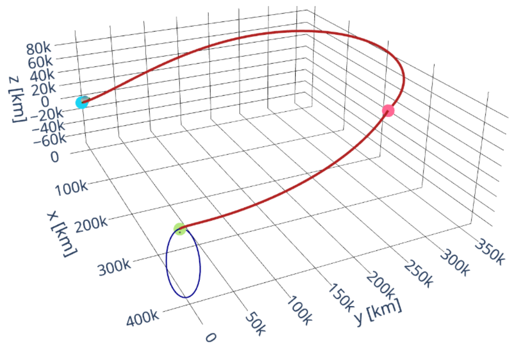

Fig. 59: Transfer trajectory to NRHO 4:1 for TOF = 10 days and 3 impulses

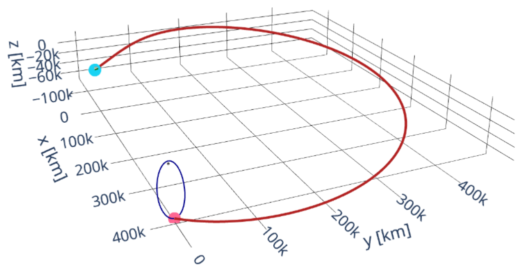

Fig. 60: Transfer trajectory to NRHO 4:1 for TOF = 12 days and 2 impulses

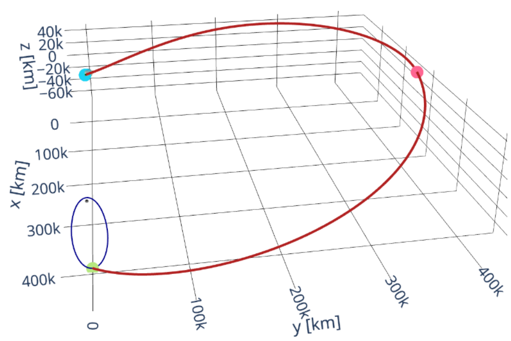

Fig. 61: Transfer trajectory to NRHO 4:1 for TOF = 12 days and 3 impulses

As can be gathered from table II and figures 26 to 33, for the transfer up to the 1:1 Butterfly, the total cost of the manoeuvre is reduced when increasing the TOF up to 10 days. In addition, the y-component of the trajectory increases from 100,000 km in the case of 4 days of flight to 400,000 km in the case of 12 days of flight. On the other hand, it can be noticed that the best transfers to this orbit are those towards the periapsis.

Furthermore, from table III and figures 34 to 42, for the transfer up to the 3:2 Butterfly, the total cost of the manoeuvre is reduced when increasing the TOF up to 12 days. In addition, the y-component of the trajectory increases from 100,000 km in the case of 4 days of flight to 400,000 km in the case of 12 days of flight. However, this component is reduced when inserting the third impulse, being drastically reduced for low TOF and slightly reduced for longer periods.

On the other hand, from table IV and figures 43 to 53, it can be noted that the Butterfly 2:1 has a very similar behaviour to the Butterfly 3:2, both in terms of cost and trajectory shape (y and z components).

When moving to the 4:1 NRHO transfer, from table V and figures 54 to 61, the total cost of the manoeuvre is also generally reduced when increasing the TOF. It is remarkable that the optimal transfers for the times of flight studied in this article occur indistinctly towards the apsides of the orbit in consideration. In this case, there is hardly any variation in the y-component of the transfer trajectory when adding a third impulse, which contrasts with the results obtained for the most of the Butterfly family.

From the data obtained in this section, it could be concluded that for short transfer missions, ideal for manned missions, the cost of direct transfer would be reduced by increasing the flight time from 1 up to 2 weeks. However, the results show that the difference would not be excessive, and that it would therefore be feasible to study a direct mission with a flight time of around one week. Furthermore, the transfer costs to a Butterfly or an NRHO are almost identical, which makes sense since the arrival states are very similar. Therefore, to benefit from the Butterfly family's instability in terms of transfer costs, a mission with a much longer time of flight (and therefore only unmanned missions)should be considered, by making use of the arrival manifold structures, which will be detailed in the next section.

VI. Possible practical applications for Butterfly orbits

In the following section, the implementation of Butterfly orbits in practical applications will be explored, considering their unique characteristics and the advantages they offer over other orbit types. Various renowned missions will be selected, and a comparison will be made between the initial orbit employed in each mission and the corresponding Butterfly orbit. This analysis will shed light on the benefits and potential applications of Butterfly orbits in real-world scenarios.

Taking into account the common characteristics of NRHO and Butterfly orbits, our attention will be directed towards missions that specifically employ NRHOs. As attributes such as resonance properties, eclipse avoidance and lunar coverage of the South Pole are inherent to both types of orbits, they will not be discussed in detail. Nevertheless, it is worth highlighting that these characteristics still offer advantages compared to the majority of other orbit types such as lunar orbits.

A. NRHO practical applications

1) Artemis mission: The Artemis mission, a joint endeavor between European Space Agency (ESA) and NASA, aims to facilitate the return of humans to the Moon [18]. A key to this mission is the lunar gateway, a small space station intended to orbit the Moon. The lunar gateway serves as a staging point for lunar surface missions and offers a platform for scientific research. To achieve this, the lunar gateway will be placed in a NRHO around the Moon [19]. Additionally, a transfer from a parking Earth orbit to the NRHO configuration will be executed[9].

The Gateway orbit is planned to be a highly-elliptical seven-day NRHO around the Moon, which would bring the small space station within 3,000 km of the lunar north pole at closest approach and as far away as 70,000 km over the lunar south pole [20] [21] [22]. Among the advantages of the NRHO orbit, which have made it the orbit of choice to host the lunar gateway, the following can be highlighted:

- Long-Term Stability: NRHO orbits exhibit better long-term stability, requiring minimal station-keeping maneuvers to maintain the desired position of the gateway.
- Mission Experience: NRHO orbits have been extensively studied and utilized in previous lunar missions, particularly within the Apollo program. The experience gained from these missions can inform decision-making and operations.
- Targeted Coverage of Points of Interest: NRHO orbits can be optimized to provide better coverage of specific points of interest on the lunar surface, aligning with mission objectives and scientific priorities.

2) Lunar Reconnaissance Orbiter mission: Launched in 2009 by NASA, the Lunar Reconnaissance Orbiter (LRO) is a robotic spacecraft specifically designed to collect data about the lunar environment and create high-resolution maps of the Moon's surface [23].

To fulfill its mission objectives, the LRO spacecraft was placed into a Near Rectilinear Halo Orbit (NRHO) around the EM-L1 with a perilune radius of about 50 kilometers above the lunar surface. It was launched the 18^{th} of June of 2009 and inserted into the orbit 5 days later. This orbit was carefully selected to ensure that the spacecraft maintained a nearly constant view of the lunar surface, which proved advantageous for conducting detailed observations and precise mapping activities. [24]

The utilization of the NRHO for the LRO mission offered several notable benefits. Firstly, it provided a stable and predictable orbit, reducing the frequency of orbital corrections required. As a result, the spacecraft could primarily focus on its scientific goals without significant interruptions or excessive fuel consumption. Additionally, the NRHO allowed for improved coverage of the lunar surface, enabling the LRO to capture high-resolution images and acquire valuable scientific data.

B. Possible Butterfly practical applications

Throughout this article, the most important characteristics of the Butterfly orbital family have been discussed. In the following, a recapitulation of the attributes that make the butterfly orbits great candidates for hosting future lunar missions will be given:

- Enhanced Flexibility: Due to their lower stability, butterfly orbits offer greater flexibility in terms of station keeping and maneuverability. This allows for easier reconfiguration of the satellite's position and orientation as required.
- Improved Lunar Surface Coverage: Butterfly orbits allow for better coverage of the lunar surface, facilitating comprehensive observation and exploration of various regions.
- Transfer Costs: As have been seen in the previous section, the direct transfer cost (based on the Lambert transfer) to butterfly orbits and NRHOs is practically identical, so there would be no clear advantage to propose the use of one over the other simply on this basis.

However, in terms of cost reduction, the employment of stable and unstable manifolds is an additional advantage offered by Butterfly orbits, which has not been explored in this study. In the CR3BP, some periodic orbits are unstable and, therefore, possess both stable and unstable invariant manifolds. [6] In this application, invariant manifolds are six-dimensional structures that govern the flow toward and away from an unstable periodic orbit; leveraging this natural dynamical structure allows transfers to and from the orbit for relatively minor maneuver cost. Manifold structures are, therefore, often a basis for transfer design techniques. Orbit stability, as determined from the eigenvalues of the monodromy matrix determines the types of manifold structures that an orbit possesses. Unstable eigenvalues ($|\lambda_i| > 1$) correspond to unstable manifold structures that depart a periodic orbit, likewise, stable eigenvalues ($|\lambda_i| < 1$) correspond to stable manifold structures that flow into a periodic orbit [25] [26].

Manifolds offer pathways for arrival at and departure from unstable periodic orbits. One of the challenges associated with transferring to/from NRHOs (as well as other stable or nearly-stable periodic orbits like DROs) is their lack of useful arrivals/departures structures, which evolve too slowly for practical application. Butterfly orbits characterized by higher stability indices can effectively utilize stable and unstable manifolds, thereby facilitating fuel-saving strategies and enabling low-energy transfer possibilities.

VII. Final remarks

Butterfly orbits are identified as viable candidate orbits for a habitat spacecraft in cis-lunar space. In this investigation, properties of the Butterflies that lead to their desirable characteristics are explored. They posses favorable eclipse avoidance and lunar coverage properties. In terms of transfer costs, preliminary transfer studies indicate that the butterflies are accessible from LEO for a relatively low-cost and short time of flight, they present the same direct transfer cost as a NRHO, and would therefore be equally well suited to host a crewed mission. Additionally, for longer duration unmanned missions, the use of manifold structures could be studied, which would differentiate the transfer cost to an NRHO and a Butterfly, since the latter, being more unstable, would present manifolds that could be used for practical application, which is not the case with NRHOs.

[9] It's important to note that the Artemis mission is a multi-phase endeavor with multiple missions planned, each with its own specific orbital requirements. The orbits used can vary depending on mission objectives, spacecraft capabilities, and operational considerations.

Therefore, for future work on butterfly orbits, the natural continuation of this study would be to compute stable and unstable manifold structures, or, more specifically, trajectories that lie along these manifold surfaces, in butterfly orbits. In this way, an overall comparison of the total mission cost could be made, weighing station keeping costs against the transfer cost in order to optimise the total mission cost.

REFERENCES

[1] NASA. The Artemis Accords.

[2] Emily M.Zimovan-Spreen, Kathleen C.Howell and Diane C.Davis *Near rectilinear halo orbits and nearby higher-period dynamical structures: orbital stability and resonance properties*, Springer Nature B.V. 2020

[3] Emily M.Zimovan-Spreen and Kathleen C.Howell *Dynamical structures nearby NHROs with applications in cislunar space*, SAAS/AIAA Astrodynamics Specialist Conference

[4] Doedel, Eusebius J., et al.*Elemental periodic orbits associated with the libration points in the circular restricted 3-body problem.*, International Journal of Bifurcation and Chaos 17.08 (2007)

[5] A.Tseloussova, S.Trofimov, M.Shirobokov and M.Ovchinnikov, *Geometric Analysis of Sun-Assisted Lunar Transfer Trajectories in the Planar Bicircular Four-Body Model*, Appl. Sci. 2023, Moscow, Russia. 2023

[6] Wang Sang Koon, Martin W. Lo, Jerrold E.Marsden and Shane D Ross.*Dynamical Systems, the Three-Body Problem and Space Mission Design*, 2011

[7] G.Gargioni, D.Alexandre, M.Peterson and K.Schroeder, *Multiple Asteroid Retrieval Mission from Lunar Orbital Platform-Gateway Using Reusable Spacecrafts*, 2019 IEEE Aerospace Conference

[8] Koon, Wang Sang, et al.*Dynamical systems, the three-body problem and space mission design.*, Equadiff 99: (In 2 Volumes). 2000.

[9] Grebow, Daniel.*Generating periodic orbits in the circular restricted three-body problem with applications to lunar south pole coverage.*, MSAA Thesis, School of Aeronautics and Astronautics

[10] E. Blazquez, T. Gateau, and S. Lizy-Destrez., *SEMpy: a Python Open-source Toolbox for Non-Keplerian Astrodynamics*, Sopot, Poland, 2021

[11] Ryan J. Whitley, Diane C. Davis, Laura M. Burke, Brian P. McCarthy, Rolfe J. Power, Melissa L.McGuire and Kathleen C.Howell *Earth-Moon Near Rectilinear Halo and Butterfly orbits for lunar surface exploration*, AAS/AIAA Astrodynamics Specialist. Snowbird, Utah, August 2018

[12] Bolliger, Matthew John. *Cislunar mission design: Transfers linking near rectilinear halo orbits and the butterfly family.*, Diss. Purdue University Graduate School, 2019.

[13] S. Nozette. C. Lichtenberg, P. Spudis, R. Bonner, W. Ort. E. Maleret, M. Robinson, and E. Shoemaker, *The Clementine Bistatic Radar Experiment.*, Science, Vol. 274, Issue 5292, 1996, pp. 1495- 1498

[14] Grebow, Daniel J., et al.*Multibody orbit architectures for lunar south pole coverage*, Journal of Spacecraft and Rockets 45.2 (2008): 344-358.

[15] R. Wilson and K. Howell, *Trajectory Design in the Sun-Earth-Moon System Using Multiple Lunar Gravity Assists*, Journal of Spacecraft and Rockets, Vol. 35, No. 2, March-April 1998

[16] NASA, *Reference Frames Coordinate Systems - NASA / NAIF*, https://naif.jpl.nasa.gov/pub/naif/toolkit_docs/Tutorials/pdf/individual_docs/17_frames_and_coordinate_systems.pdf

[17] G. Gemignani, G. Bucchioni, S. Lizy-Destrez, M. Innocenti, *Primer Vector Based optimal Guidance For Orbital Transfers In Cislunar Environment*, ESA GNC-ICATT 2023

[18] ESA, *Artemis I mission overview - ESA* https://blogs.esa.int/orion/2022/08/27/artemis-i-mission-overview/

[19] NASA, *Gateway Lunar Space Station Cofiguration - NASA* https://www.nasa.gov/gateway/overview

[20] ESA, *Angelic halo orbit chosen for humankind's first lunar outpost* PhysOrg, 19 July 2019, accessed 15 June 2020

[21] D. Szondy, *Halo orbit selected for Gateway space station* New Atlas. 18 July 2019

[22] J. Foust, *"NASA cubesat to test lunar Gateway orbit"*. SpaceNews. 16 September 2019

[23] NASA, *LRO Mission Overview - NASA* https://www.nasa.gov/mission_pages/LRO/overview/index.html

[24] NASA, *Lunar Reconnaissance Orbiter in-depth - NASA* https://solarsystem.nasa.gov/missions/lro/in-depth/

[25] E. M. Zimovan, *"Characteristics and Design Strategies for Near Rectilinear Halo Orbits within the Earth-Moon System"*. M.S. Thesis, School of Aeronautics and Astronautics, Purdue University, West Lafayette, Indiana, August 2017.

[26] E. M. Zimovan, K. C. Howell, and D. C. Davis, *"Near Rectilinear Halo Orbits and Their Application in Cis-Lunar Space"*. 3rd International Academy of Astronautics Conference on Dynamics and Control of Space Systems, Moscow, Russia, May 30 – June 1, 2017.

APPENDIX

A. *Earth-Butterfly transfer cost*

In this list, all the attempts that have been made in order to find the best result for the transfer, are shown. They are ordered by arrival orbit and time of flight (TOF). The numbers inside () represent the departure or arrival state in our code. On the right, the results show the number of impulses and the total transfer cost in m/s.

Butterfly 2:1

TOF= 4 days

Park(300)-But(467): 3 imp - 5148
Park(350)-But(467): 3 imp - 5041
Park(350)-But(1533): NO RESULT (time limit)
Park(350)-But(430): 3 imp - 5083
Park(370)-But(467): 3 imp - 5075
Park(370)-But(1533): 3 imp - 5329
Park(370)-But(430): 3 imp - 5119
Park(400)-But(467): 3 imp - 5313
Park(400)-But(1533): 3 imp - 5497
Park(400)-But(430): 3 imp - 5362
Park(430)-But(467): 3 imp - 5784
Park(430)-But(1533): 3 imp - 5918
Park(430)-But(430): 3 imp - 5829
Park(470)-But(467): 3 imp- 7139
Park(470)-But(1533): 3 imp - 7436
Park(470)-But(430): 3 imp - 6849
Park(500)-But(467): 3 imp - 7746
Park(500)-But(1533): 3imp - 8079
Park(500)-But(430): 3 imp - 7453
Park(530)-But(467): 3 imp - 8264
Park(530)-But(1533): 3 imp - 8697
Park(530)-But(430): 3 imp - 7979
Park(560)-But(467): 3 imp - 8590
Park(560)-But(1533): 3 imp - 9202
Park(560)-But(430): 3 imp - 8329

TOF= 7 days

Park(300)-But(467): NO RESULT (derivative at interior impulse in non zero nor continuous)
Park(350)-But(467): NO RESULT (derivative at interior impulse in non zero nor continuous)
Park(350)-But(1533): 4 imp - 5096
Park(350)-But(430): 4 imp - 5094
Park(370)-But(467): NO RESULT (time limit)
Park(370)-But(1533):NO RESULT (time limit)
Park(370)-But(430): 4 imp - 5090
Park(400)-But(467): 3 imp - 5928
Park(400)-But(1533): NO RESULT (time limit)
Park(400)-But(430): 4 imp - 5122
Park(430)-But(467): 3 imp - 5959
Park(430)-But(1533): 3 imp - 5521
Park(430)-But(430): 4 imp - 5250
Park(470)-But(467): 3 imp - 6279
Park(470)-But(1533): 3 imp - 5827
Park(470)-But(430): 4 imp - 5631
Park(500)-But(467): 3 imp - 6677
Park(500)-But(1533): 3 imp - 6254
Park(500)-But(430): 4 imp - 6043
Park(530)-But(467): 3 imp - 7093
Park(530)-But(1533): 3 imp - 6742
Park(530)-But(430): NO RESULT (derivative at interior impulse in non zero nor continuous)
Park(560)-But(467): 3 imp - 7462
Park(560)-But(1533): 3 imp - 7229
Park(560)-But(430): NO RESULT (derivative at interior impulse in non zero nor continuous)

TOF= 10 days

Park(470)-But(467): 3 imp - 5967
Park(470)-But(1533): 3 imp - 5166
Park(470)-But(430): 4 imp - 4964
Park(500)-But(467): 3 imp - 6021
Park(500)-But(1533): 3 imp - 5215
Park(500)-But(430): 4 imp - 5145
Park(530)-But(467): 3 imp - 6353
Park(530)-But(1533): 3 imp - 5569
Park(530)-But(430): 4 imp - 5488
Park(560)-But(467): 3 imp - 6720
Park(560)-But(1533): 3 imp - 6004
Park(560)-But(430): 4 imp - 5886

TOF= 12 days

Park(470)-But(467): 3 imp - 6954
Park(470)-But(1533): 4 imp - 4954
Park(470)-But(430): 4 imp - 4824
Park(500)-But(467): 3 imp - 6055
Park(500)-But(1533): 4 imp - 4903
Park(500)-But(430): 4 imp - 4828
Park(530)-But(467): 3 imp - 6068
Park(530)-But(1533): 3 imp - 5103
Park(530)-But(430): NO RESULT (time limit)
Park(560)-But(467): 3 imp - 6329
Park(560)-But(1533): 3 imp - 5404
Park(560)-But(430): 4 imp - 5326

Butterfly 3:2

TOF= 4 days

Park(300)-But(480): NO RESULT (derivative at interior impulse in non zero nor continuous)
Park(350)-But(480): 3 imp - 5031
Park(350)-But(1520): NO RESULT (derivative at interior impulse in non zero nor continuous)
Park(350)-But(339): 3 imp - 5157
Park(370)-But(480): 3 imp - 5065
Park(370)-But(1520): 3 imp - 5360
Park(370)-But(339): 3 imp - 5211
Park(400)-But(480): 3 imp - 5302
Park(400)-But(1520): 3 imp - 5523
Park(400)-But(339): 3 imp - 5462
Park(420)-But(480): 3 imp - 5593
Park(420)-But(1520): 3 imp - 5776
Park(420)-But(339): 3 imp - 5741
Park(450)-But(480): 3 imp - 6178
Park(450)-But(1520): 3 imp - 6322
Park(450)-But(339): 3 imp - 6284

Park(470)-But(480): 3 imp - 6621
Park(470)-But(1520): 3 imp - 6753
Park(470)-But(339): 3 imp - 6690
Park(500)-But(480): 3 imp - 7293
Park(500)-But(1520): 3 imp - 7431
Park(500)-But(339): 3 imp - 7303
Park(530)-But(480): 3 imp - 7893
Park(530)-But(1520): 3 imp - 8078
Park(530)-But(339): 3 imp - 7844
Park(560)-But(480): 3 imp - 8322
Park(560)-But(1520): 3 imp - 8601
Park(560)-But(339): 3 imp - 8223

TOF= 7 days

Park(350)-But(480): 3 imp - 5140
Park(350)-But(1520): NO RESULT (time limit)
Park(350)-But(339): 4 imp - 5013
Park(370)-But(480): 3 imp - 5140
Park(370)-But(1520): NO RESULT (time limit)
Park(370)-But(339): 4 imp - 5019
Park(400)-But(480): 3 imp - 5153
Park(400)-But(1520): 3 imp - 4942
Park(400)-But(339): 4 imp - 5071
Park(430)-But(480): 3 imp - 5194
Park(430)-But(1520): 3 imp - 4933
Park(430)-But(339): 3 imp - 5200
Park(470)-But(480): 3 imp - 5566
Park(470)-But(1520): 3 imp - 5277
Park(470)-But(339): 3 imp - 5537
Park(500)-But(480): 3 imp - 6015
Park(500)-But(1520): 3 imp - 5739
Park(500)-But(339): 3 imp - 5942
Park(530)-But(480): 3 imp - 6483
Park(530)-But(1520): 3 imp - 6250
Park(530)-But(339): 3 imp - 6373
Park(560)-But(480): 3 imp - 6910
Park(560)-But(1520): 3 imp - 6746
Park(560)-But(339): 3 imp - 6771

TOF= 10 days

Park(470)-But(480): 3 imp - 5303
Park(470)-But(1520): 3 imp - 4708
Park(470)-But(339): NO RESULT (derivative at interior impulse in non zero nor continuous)
Park(500)-But(480): 3 imp - 5256
Park(500)-But(1520): 3 imp - 4772
Park(500)-But(339): NO RESULT (derivative at interior impulse in non zero nor continuous)
Park(530)-But(480): 3 imp - 5644
Park(530)-But(1520): 3 imp - 5175
Park(530)-But(339): 3 imp - 5486
Park(560)-But(480): 3 imp - 6046
Park(560)-But(1520): 3 imp - 5622
Park(560)-But(339): 3 imp - 5858

TOF= 12 days

Park(470)-But(480): 3 imp - 5270
Park(470)-But(1520): 3 imp - 4705
Park(470)-But(339): 4 imp - 4738
Park(500)-But(480): 3 imp - 5257
Park(500)-But(1520): NO RESULT (derivative at interior impulse in non zero nor continuous)
Park(500)-But(339): 4 imp - 4760
Park(530)-But(480): 3 imp - 5337
Park(530)-But(1520): 3 imp - 4785
Park(530)-But(339): NO RESULT (time limit)
Park(560)-But(480): 3 imp - 5619
Park(560)-But(1520): 3 imp - 5087
Park(560)-But(339): 4 imp - 5304

Butterfly 1:1

TOF= 4 days

Park(350)-But(504): NO RESULT (time limit)
Park(350)-But(1499): NO RESULT (derivative at interior impulse in non zero nor continuous)
Park(350)-But(255): 3 imp - 5214
Park(370)-But(504): 3 imp - 4812
Park(370)-But(1499): 3 imp - 4985
Park(370)-But(255): 3 imp - 5294
Park(400)-But(504): 3 imp - 4977
Park(400)-But(1499): 3 imp - 5230
Park(400)-But(255): 3 imp - 5589
Park(430)-But(504): 3 imp - 5430
Park(430)-But(1499): 3 imp - 5753
Park(430)-But(255): 3 imp - 6071
Park(470)-But(504): 3 imp - 6312
Park(470)-But(1499): 3 imp - 6665
Park(470)-But(255): 3 imp - 6874

TOF= 7 days

Park(350)-But(504): 3 imp - 4912
Park(350)-But(1499): NO RESULT (derivative at interior impulse in non zero nor continuous)
Park(350)-But(255): 4 imp - 5011
Park(370)-But(504): 3 imp - 4886
Park(370)-But(1499): NO RESULT (time limit)
Park(370)-But(255): 4 imp - 4991
Park(400)-But(504): 3 imp -4845
Park(400)-But(1499): 3 imp - 4700
Park(400)-But(255): 3 imp - 5146
Park(430)-But(504): 3 imp - 4845
Park(430)-But(1499): 3 imp - 4745
Park(430)-But(255): 3 imp - 5221
Park(470)-But(504): 3 imp - 5210
Park(470)-But(1499): 3 imp - 5218
Park(470)-But(255): 3 imp - 5605

TOF= 10 days

Park(400)-But(504): 3 imp - 4969
Park(400)-But(1499): NO RESULT (derivative at interior impulse in non zero nor continuous)
Park(400)-But(255): NO RESULT (derivative at interior impulse in non zero nor continuous)
Park(430)-But(504): 3 imp - 4933
Park(430)-But(1499): 3 imp - 4648
Park(430)-But(255): 4 imp - 4742
Park(470)-But(504): 3 imp - 4905
Park(470)-But(1499): 3 imp - 4578
Park(470)-But(255): NO RESULT (time limit)

Park(500)-But(504): 3 imp - 5010
Park(500)-But(1499): 3 imp - 4813
Park(500)-But(255): 4 imp - 5024
TOF= 12 days
Park(400)-But(504): 3 imp - 5011
Park(400)-But(1499): NO RESULT (derivative at interior impulse in non zero nor continuous)
Park(400)-But(255): 4 imp - 4813
Park(430)-But(504): 3 imp - 4972
Park(430)-But(1499): NO RESULT (derivative at interior impulse in non zero nor continuous)
Park(430)-But(255): 4 imp - 4753
Park(470)-But(504): 3 imp - 4962
Park(470)-But(1499): NO RESULT (derivative at interior impulse in non zero nor continuous)
Park(470)-But(255): 4 imp - 4679
Park(500)-But(504): 3 imp - 5001
Park(500)-But(1499): 3 imp - 4630
Park(500)-But(255): 4 imp - 4674

NRHO

TOF= 4 days
Park(400)-But(989): 3 imp - 5130
Park(430)-But(500): NO RESULT
Park(430)-But(0): 3 imp - 5084
Park(430)-But(11): 3 imp -5086
Park(430)-But(989): 3 imp - 5187
Park(470)-But(500): 3 imp - 7513
Park(470)-But(0): 3 imp - 6591
Park(470)-But(11): 3 imp - 6595
Park(470)-But(989): 3 imp - 6903
Park(500)-But(500): 3 imp - 7513
Park(500)-But(0): 3 imp - 7167
Park(500)-But(11): 3 imp - 7170
Park(500)-But(989): 3 imp - 7515
Park(530)-But(500): 3 imp - 8104
Park(530)-But(0): 3 imp - 7698
Park(530)-But(11): 3 imp - 7701
Park(530)-But(989): 3 imp - 8096
Park(560)-But(500): NO RESULT (derivative at interior impulse in non zero nor continuous)
Park(560)-But(0): 3 imp - 8132
Park(560)-But(11): 3 imp - 8133
Park(560)-But(989): 3 imp - 8495
TOF= 7 days
Park(470)-But(500): 3 imp - 5265
Park(470)-But(0): 3 imp - 5387
Park(470)-But(11): 3 imp - 5388
Park(470)-But(989): 3 imp - 5476
Park(500)-But(500): NO RESULT (derivative at interior impulse in non zero nor continuous)
Park(500)-But(0): 3 imp - 5749
Park(500)-But(11): 3 imp - 5751
Park(500)-But(989): 3 imp - 5849
Park(530)-But(500): 3 imp - 6768
Park(530)-But(0): 3 imp - 6166
Park(530)-But(11): 3 imp - 6167
Park(530)-But(989): 3 imp - 6290
Park(560)-But(500): 3 imp - 7210
Park(560)-But(0): 3 imp - 6576
Park(560)-But(11): 3 imp - 6576
Park(560)-But(989): 3 imp - 6733
TOF= 10 days
Park(470)-But(500): 3 imp - 5481
Park(470)-But(0): 3 imp - 4908
Park(470)-But(11): 3 imp - 4909
Park(470)-But(989): 3 imp - 4950
Park(500)-But(500): 3 imp - 5562
Park(500)-But(0): 3 imp - 4999
Park(500)-But(11): 3 imp - 4999
Park(500)-But(989): 3 imp - 5029
Park(530)-But(500): 3 imp - 5898
Park(530)-But(0): 3 imp - 5256
Park(530)-But(11): 3 imp - 5256
Park(530)-But(989): 3 imp - 5288
Park(560)-But(500): 3 imp - 6310
Park(560)-But(0): 3 imp - 5617
Park(560)-But(11): 3 imp - 5617
Park(560)-But(989): 3 imp - 5670
TOF= 12 days
Park(400)-But(500): 3 imp - 5194
Park(400)-But(0): 4 imp - 4600
Park(400)-But(11): 4 imp - 4597
Park(400)-But(989): 4 imp - 4980
Park(470)-But(500): NO RESULT (too close to the moon)
Park(470)-But(0): 3 imp - 4845
Park(470)-But(11): 3 imp - 4846
Park(470)-But(989): 3 imp - 4860
Park(500)-But(500): 3 imp - 5545
Park(500)-But(0): 3 imp - 4831
Park(500)-But(11): 3 imp - 4831
Park(500)-But(989): 3 imp - 4846
Park(530)-But(500): 3 imp - 5571
Park(530)-But(0): 3 imp - 4864
Park(530)-But(11): 3 imp - 4863
Park(530)-But(989): 3 imp - 4872